AD NUMBER

AD848543

NEW LIMITATION CHANGE

TO

Approved for public release, distribution unlimited

FROM

Distribution authorized to DoD only; Test and Evaluation; NOV 1968. Other requests shall be referred to Office of Naval Research, Code 463, One Liberty Center, 875 North Randolph Street, Arlington, VA 22203-1995.

AUTHORITY

onr ltr, 9 nov 1973

ANTENNA STUDY FOR D/F APPLICATION

(Semi-Annual Progress Report)
1968 January 1 to 1968 June 30

DSD R-219

Prepared Under
Office of Naval Research
Contract NOnr 4798(00)
Contract Authority No. NR 259-051/2-18-66
for
U.S. Marine Corps
(R and D Project CS 454 and CS 471)

1968 November

SURC

DISCLAIMER NOTICE

**THIS DOCUMENT IS BEST QUALITY
PRACTICABLE. THE COPY FURNISHED
TO DTIC CONTAINED A SIGNIFICANT
NUMBER OF PAGES WHICH DO NOT
REPRODUCE LEGIBLY.**

⑥

ANTENNA STUDY FOR D/F APPLICATION.

⑨ Semi-Annual Progress Report. 1 Jan – 30 Jun 68

1968 January 1 to 1968 June 30

⑭ DSD-R-219

Prepared Under
Office of Naval Research
Contract NOnr-4798(00)   ⑮ Nonr-4798(00)
Contract Authority № ⑯ NR-259-051
R/D-CS-454
U.S. Marine Corps.
(R and D Project CS 454 and CS 471)

⑩
Richard G. Russell,
Stephen E. Cooper
Harvey K. Schuman

1968 November   ⑪ Nov 68   ⑫ 73 p.

DEFENSE SYSTEMS DIVISION

SYRACUSE UNIVERSITY RESEARCH CORPORATION

i

1473

339 853

TABLE OF CONTENTS (U)

LIST OF ILLUSTRATIONS (U)

PURPOSE (U)

The Contractor shall furnish the necessary personnel and facilities for
and, in accordance with instructions issued by the Scientific Officer or
his authorized representative, shall conduct an applied research pro-
gram in electronic warfare direction finding techniques:

Against HF (1-30 MHz) radio signals to significantly improve
the D/F accuracy achievable with today's field multipath signals.
Specifically, to devise and demonstrate a transportable automated
D/F antenna (and associated electronics for data processing) im-
mune to interferring signals and external RF noise. In particular,
this program includes the following:

1. Study and conduct second-order error analysis of data pro-
   cessing methods and complete the antenna concept analysis.

2. Conduct circuit experiments to determine the feasibility of
   goniometer, broadband receiver and broadband data processing
   concepts.

ABSTRACT (U)

The feasibility of utilization of a short dipole, elevated array has been demonstrated on ground-wave signals and sky-wave signals. The feasibility of sky-wave ranging has also been demonstrated. Theoretical and experimental results are included.

A data package has been submitted for the Interim Replacement for the AN/TRD-21 Antenna System.

CONFERENCES (U)

Date: 2 May 1968
Place: Syracuse University Research Corporation, Syracuse, N.Y.
Attendees: Mr. J. Fischer, ONR
             Mr. G. LaTourette, DSD

Subject: HF D/F Briefing

Date: 7 May 1968
Place: Syracuse University Research Corporation, Syracuse, N.Y.
Attendees: Mr. A. F. L. Rocke, Intercept Research Inc.
             Mr. M. Riddle, Arvin Industries
             Mr. G. LaTourette, DSD
             Mr. R. Russell, DSD

Subject: Conference on Twin Front End Concepts

Date: 22-23 May 1968
Place: Syracuse University Research Corporation, Syracuse, N.Y.
Attendees: Maj. F. W. Martino, USMC (Code A02F)
             Capt. J. S. Picken, U.S. Army
             Mr. J. M. DelVecchio, U. S. Army
             Mr. M. Weiner, USAECOM
             Dr. A. D. Bailey, University of Illinois
             Dr. J. D. Dyson, University of Illinois
             Dr. E. W. Ernst, University of Illinois
             Mr. D. Travers, SRI
             Mr. W. M. Sherill, SRI
             Mr. N. C. Gerson, Mitre
             Dr. B. E. Simmons, ASD
             Mr. J. Cummins, DSD
             Mr. G. LaTourette, DSD
             Mr. R. Russell, DSD

Subject: HF D/F Concepts for Marine Corps AMPHIBIOUS HF
             D/F System

Section I

CW D/F -- INTERIM REPLACEMENT FOR AN/TRD-21 (U)

Work has been completed on the elevated H-Adcock array that will replace the monopole array used in the AN/TRD-21 D/F System. A data package was submitted to the Marine Corps.

1. D/F BEARING TESTS (U)

A comparison of bearing accuracy for the AN/TRD-21 D/F set and the interim array was made as a function of azimuth angle. This test was conducted for a limited number of bearing cuts and more tests should be conducted. Table 1 shows the results of the comparison. Figure 1 illustrates the number of occurrences of a bearing angle $\Delta \phi$.

2. OCTANTAL ERROR (U)

The bearing observed on the azimuth indicator of the AN/TRD-21 HF D/F System is

$$\phi_p \cong \tan^{-1}\left[\tan\phi + \epsilon \sec^2\phi\right]$$

where

ϕ_p = position of propellor peak observed on the azimuth-indicator

ϕ = true bearing

$\epsilon = \left(\dfrac{\pi d}{\lambda}\right)^2 \dfrac{\sin 4\phi}{24}$

d = element spacing

λ = free space wavelength

ϕ_g = octantal error

Russell, R.G., et al, "Antenna Study for D/F Application", DSD R-192 (Semi-Annual Progress Report), 1 July 1967 to 21 December 1967, Contract NOnr 4798(00), February 1968, Section I-B.

TABLE 1 Comparison of Bearing Accuracy (U)

Frequency (MHz)	Bearing Reading from North (degrees)	Octantal Error (degrees)	Corrected Bearing (degrees)	True Location (degrees)	Error $\Delta\phi$ (degrees)	Array
29.906	9.0	-5.5	3.5	1.0	+2.5	Elevated H
21.820	4.5	-2.0	2.5		+1.5	
14.550	358.5	0.0	358.5		-2.5	
9.750	2.0	-0.5	1.5		+0.5	
6.768	1.0		1.0		0.0	
3.810	4.5		4.5		+3.5	
2.450	357.0		357.0		-4.0	
29.906	9.0	-4.0	5.0		+4.0	21 Antenna System
21.820	0.5	0.0	0.5		-0.5	
14.550	0.5	0.0	0.5		-0.5	
9.750	358.0	0.0	358.0		-3.0	
6.768	2.5		2.5		+1.5	
3.810	6.0		6.0		+5.0	
2.450	9.5		9.5		+8.5	
29.000	52.0	+9.5	61.5	59.5	+2.0	Elevated H
21.000	60.0	+5.0	65.0		+5.5	
14.000	60.0	+2.0	62.0		+2.5	
9.000	57.5	+0.5	58.0		-1.5	
6.000	48.0		48.0		-11.5	
3.000	57.5		57.5		-2.0	
2.000	63.5		63.5		+4.0	

2

TABLE 1   Comparison of Bearing Accuracy (U) (cont'd)

Frequency (MHz)	Bearing Reading from North (degrees)	Octantal Error (degrees)	Corrected Bearing (degrees)	True Location (degrees)	Error Δφ (degrees)	Array
29.000	41.5	-4.5	37.0		22.5	21 Antenna System
21.000	58.0	+5.0	63.0		+3.5	
14.000	61.0	+1.5	62.5		+3.0	
9.000	61.0	+1.0	62.0		+2.5	
6.000	57.0		57.0		-2.5	
3.000	60.0		60.0		+0.5	
2.000	61.0		61.0		+1.5	
29.000	102.5	-6.5	95.5	45.0	0.5	Elevated H
21.000	96.0	-2.0	94.0		-1.0	
14.000	95.0	-1.0	94.0		-1.0	
9.000	100.5	-1.0	99.5		+4.5	
6.000	93.5		93.5		-1.5	
3.000	100.0		100.0		+5.0	
2.000	100.0		100.0		+5.0	
29.000	104.0	-6.0	98.0		+3.0	21 Antenna System
21.000	106.0	-4.0	102.0		+7.0	
14.000	104.5	-0.5	104.0		+9.0	
9.000	100.5	-0.5	100.0		+5.0	
6.000	95.5		95.5		+0.5	
3.000	95.0		95.0		0.0	
2.000	94.5		94.5		-0.5	

TABLE 1 Comparison of Bearing Accuracy (U) (cont'd)

Frequency (MHz)	Bearing Reading from North (degrees)	Octantal Error (degrees)	Corrected Bearing (degrees)	True Location (degrees)	Error Δφ (degrees)	Array
29.000	137.5	+4.5	142.0	138.0	+ 4.0	Elevated H
21.000	142.0	+3.5	145.5		+ 7.5	
14.000	145.0	+1.0	146.0		+ 8.0	
9.000	146.0	+1.0	147.0		+ 9.0	
6.000	118.5		118.5		-19.5	
3.000	127.5		127.5		-10.5	
2.000	133.5		133.5		- 4.5	
29.000	143.0	+9.0	152.0		+14.0	21 Antenna System
21.000	144.0	+4.0	148.0		+10.0	
14.000	150.5	+1.5	152.0		+14.0	
9.000	147.5	+0.5	148.0		+10.0	
6.000	144.0		144.0		+ 6.0	
3.000	133.5		133.5		- 4.5	
2.000	133.5		133.5		- 4.5	
29.000	185.5	-3.0	182.5	187.0	- 4.5	Elevated H
21.000	192.5	-3.5	189.0		+ 2.0	
14.000	185.0	-1.0	184.0		- 3.0	
9.000	185.5	-0.5	185.0		- 2.0	
6.000	185.0		186.0		- 1.0	
3.000	185.5		185.5		- 1.5	
2.000	179.5		179.5		- 7.5	

TABLE 1   Comparison of Bearing Accuracy (U) (cont'd)

Frequency (MHz)	Bearing Reading from North (degrees)	Octantal Error (degrees)	Corrected Bearing (degrees)	True Location (degrees)	Error Δφ (degrees)	Array
29.000	198.0	-7.5	190.5		+ 3.5	21 Antenna System
21.000	198.0	-4.0	194.0		+ 7.0	
14.000	204.0	-1.5	202.5		+15.5	
9.000	200.5	-1.0	199.5		+12.5	
6.000	185.5	-1.0	185.5		- 1.5	
3.000	184.5		184.5		- 2.5	
2.000	187.0		187.0		0.0	
29.000	228.5	+5.5	234.0	226.0	+ 8.0	Elevated H
21.000	229.0	+2.0	231.0		+ 5.0	
14.000	225.0	0.0	225.0		- 1.0	
9.000	229.0	+0.5	229.5		+ 3.5	
6.000	208.5		208.5		-17.5	
3.000	210.0		210.0		-16.0	
2.000	214.0		214.0		-12.0	
29.000	224.0	-1.5	222.5		- 3.5	21 Antenna System
21.000	239.0	+5.0	244.0		+18.0	
14.000	242.0	+1.5	243.5		+17.5	
9.000	240.5	+1.0	241.5		+15.5	
6.000	227.0		227.0		+ 1.0	
3.000	225.5		225.5		0.5	
2.000	226.5		226.5		+ 0.5	

5

TABLE 1   Comparison of Bearing Accuracy (U) (cont'd)

Frequency (MHz)	Bearing Reading from North (degrees)	Octantal Error (degrees)	Corrected Bearing (degrees)	True Location (degrees)	Error Δφ (degrees)	Array
29.000	281.0	-6.0	275.0	273.5	+ 1.5	Elevated H
21.000	277.0	-2.5	274.5		+ 1.0	
14.000	281.0	-0.5	280.5		+ 7.0	
9.000	277.0	-0.5	76.5		+ 3.0	
6.000	264.0		264.0		- 9.5	
3.000	263.5		263.5		-10.0	
2.000	254.0		254.0		-19.5	
29.000	265.0	+2.0	267.0		- 3.5	21 Antenna System
21.000	270.0	0.0	270.0		- 3.5	
14.000	271.0	0.0	271.0		- 2.5	
9.000	270.0	0.0	270.0		- 3.5	
6.000	267.5		267.5		- 6.0	
3.000	263.0		263.0		-10.5	
2.000	264.5		264.5		- 9.0	
29.000	315.5	+1.0	316.5	328.0	-11.5	Elevated H
21.000	326.0	+4.5	330.5		+ 2.5	
14.000	323.5	+1.0	324.5		- 3.5	
9.000	334.0	+1.0	335.0		+ 7.0	
6.000	329.5		329.5		+ 1.5	
3.000	324.0		324.0		- 4.0	
2.000	317.0		317.0		-11.0	

TABLE 1 Comparison of Bearing Accuracy (U) (cont'd)

Frequency (MHz)	Bearing Reading from North (degrees)	Octantal Error (degrees)	Corrected Bearing (degrees)	True Location (degrees)	Error Δφ (degrees)	Array
29.000	323.5	+9.5	333.0		+5.0	21 Antenna System
21.000	323.0	+3.5	326.5		-1.5	
14.000	323.9	+1.0	324.5		-3.5	
9.000	329.5	+1.0	330.5		+2.5	
6.000	321.5		321.5		-6.5	
3.000	326.5		326.6		-1.5	
2.000	334.0		334.0		+6.0	

7
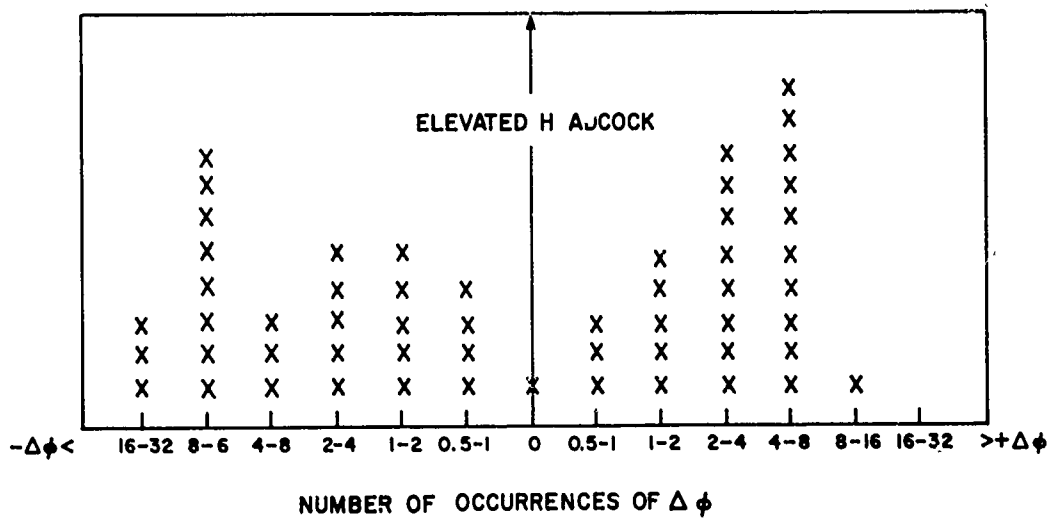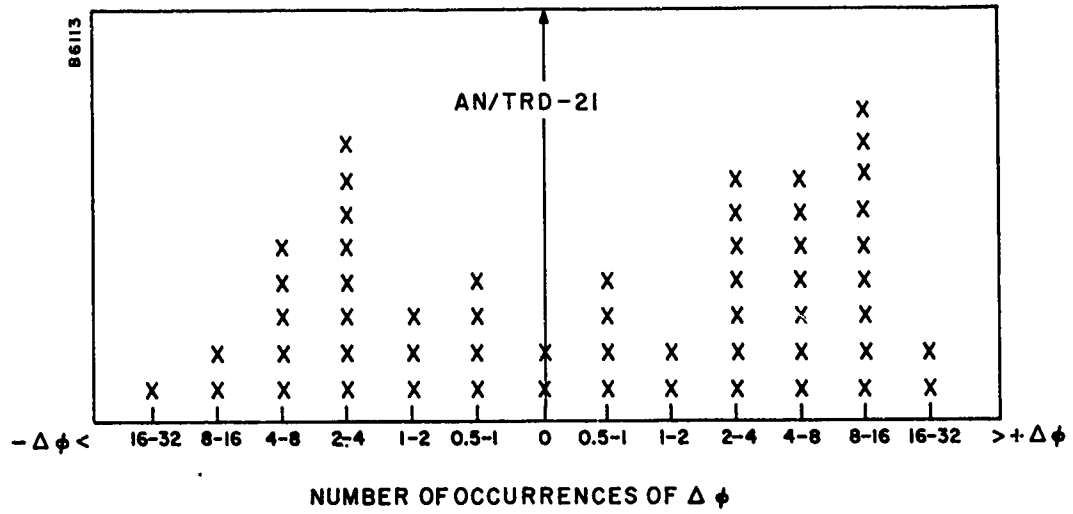
FIGURE 1   Number of Occurrences of $\Delta\phi$ (U)

$$\phi_g = \phi - \phi_p$$

$$\phi_g = \phi - \tan^{-1}\left[\tan\phi + \epsilon \sec^2\phi\right]$$

The octantal error is noted to be a function of element spacing, RF frequency, and true azimuth angle of the RF signal. An SDS Digital Computer was used to plot the octantal error as a function of observed bearing over the HF range.

The results of the plot are shown in Figure 2.

9
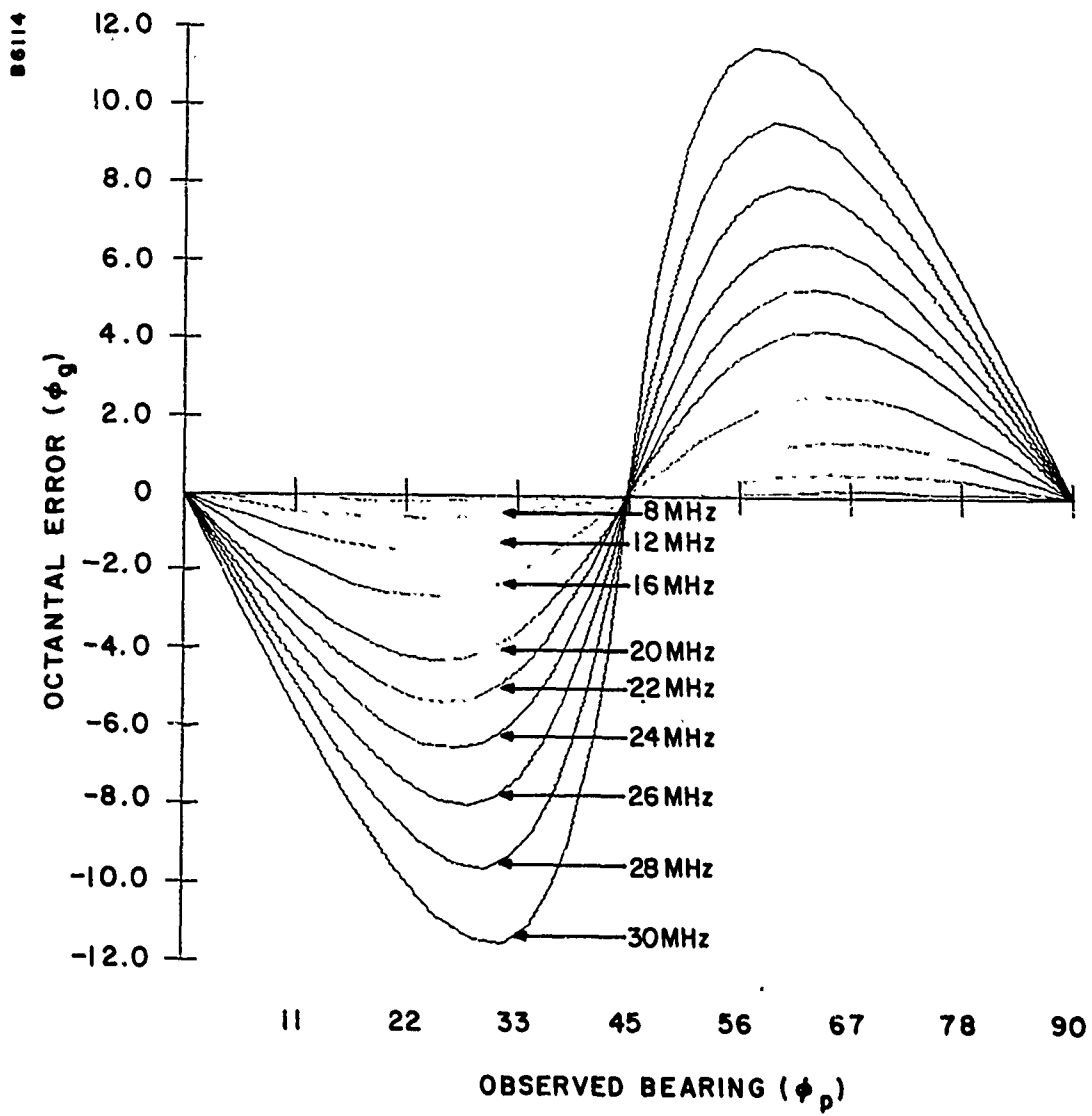
FIGURE 2   Observed Bearing (ϕ_p) (U)

10

Section II

SKY-WAVE FEASIBILITY STUDY (U)

1.   INTRODUCTION (U)

Measuring the elevational angle of a sky-wave to determine range information has been shown to be feasible using a small array with an automated system.   The range of operation will be 80 to 500 km with a range accuracy better than $\pm$ 10 per cent range.

The approach used was to measure the ionospheric height at the receiver location and to measure the elevational angle of arrival thus leading to the range by solving the triangle.   Over the range of 80 to 500 km, the flat-earth approximation is valid.   Curved-earth equations were used on all experimental ranging data processed in work at SURC[2].   The problems encountered are:

      a.   Ionospheric behavior

      b.   Measurement requirements

The conclusions reached were:

      a.   Range bracket saves problem

      b.   Additional check data desirable

The contents of the report which follows will cover:

      a.   Permissible ionospheric misbehavior

      b.   Ray measurement analysis and data

      c.   Planned follow-on work

----

[2] Boyko, L., Carmichael, J., Cooper S., Cummins, J., Schuman, H., "Antenna Study for D/F Application", DSD R-193, (Interim Report), Contract NOnr 4798(00), October, 1968.

11

2. IONOSPHERIC BEHAVIOR (U)

a. Introduction

The purpose of this section is to present and evaluate the effects of the ionosphere on various modes of sky-wave propagation. Some major parameters used in determining and describing the characteristics of the ionosphere are:

(1) Layer height

(2) Electron density

(3) Layer absorption

(4) Time variations

    (a) Diurnal

    (b) Seasonal

(5) Gross spatial variations

    (a) Polar

    (b) Temperature

    (c) Equatorial

All factors are markedly influenced by solar activity.

Figure 4 shows the ionospheric layers of most interest concerning ionospheric propagation. A flat-earth description usually is adequate at short ranges.

Figure 5 displays some of the notation used throughout this section. Unless otherwise specified the letter "F" will refer to the F_2 layer.

In this report reliance will be placed on the ITSA prediction technique[3] which primarily considers HF reflection from the E and F layers and absorption from the D layer.

----

[3] Lucas, D. L. , Haydon, G. W. , and Staff, "Predicting Statistical Performance Indexes for High Frequency Ionospheric Telecommunication Systems", Environmental Sciences Services and Aeronomy, Frequency Utilization Section, ESSA Technical Report, August, 1966.
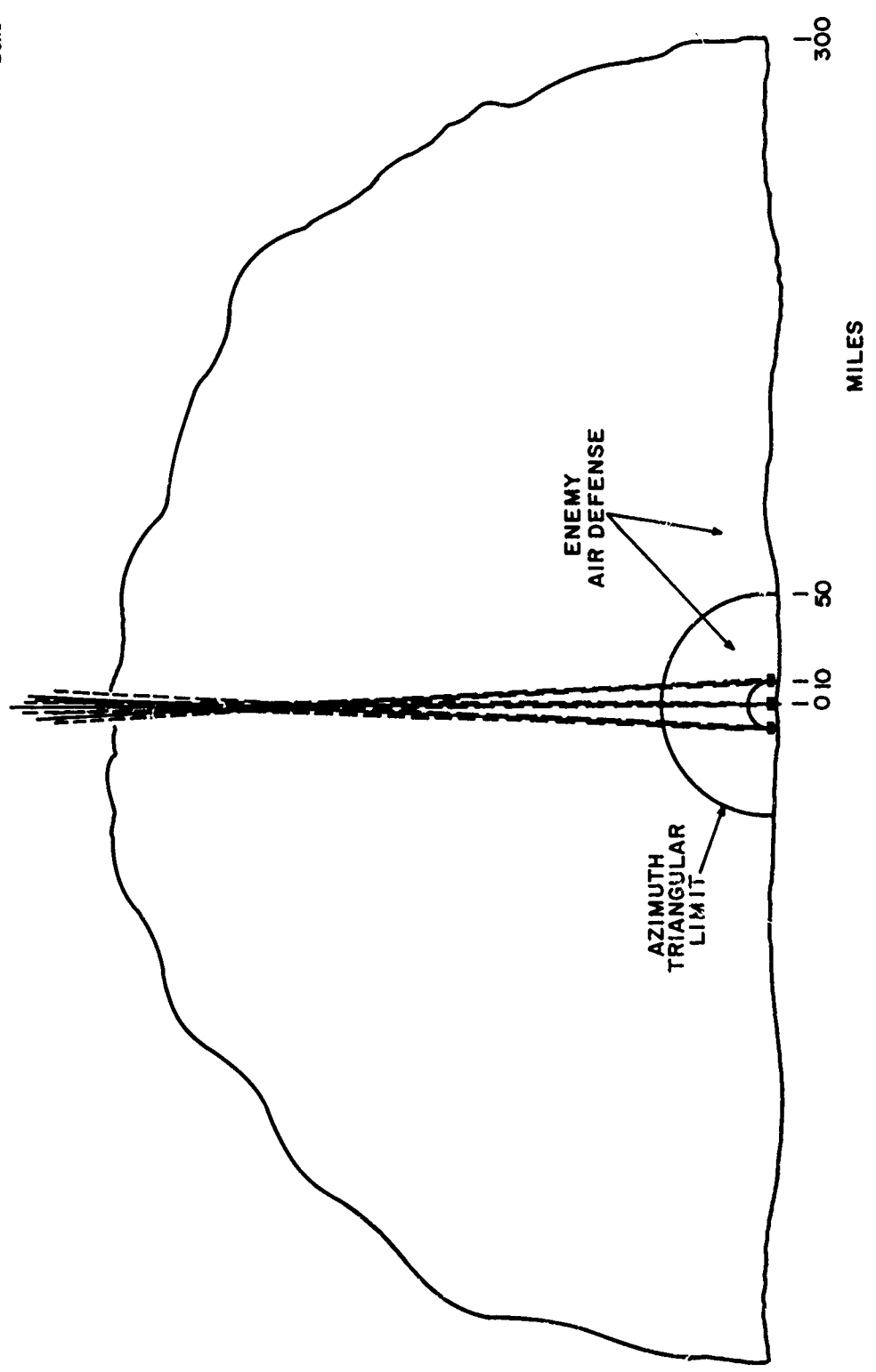
FIGURE 3   Short Base-Line Operation (U)

13

A6050
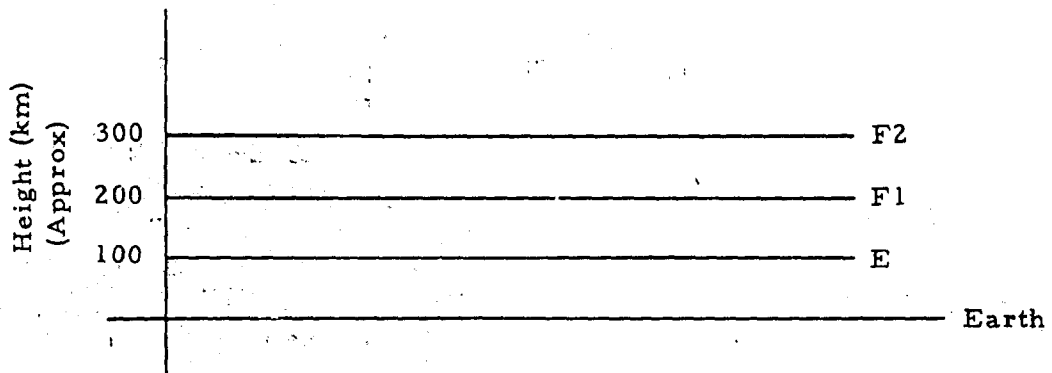
FIGURE 4   Some of the Important Ionospheric Levels and
Their Approximate Virtual Heights Above the
Earth's Surface (U)
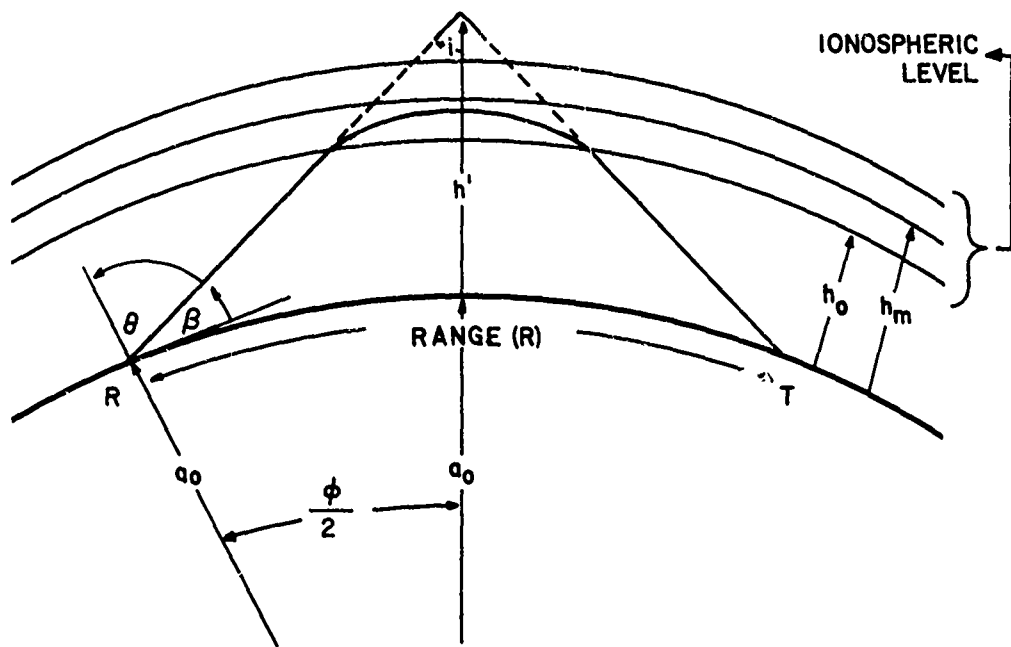
FIGURE 5 Geometry and Notation Showing One-Hop
Propagation (U)

15

b. Tools Available to Operator

The following information is available to the operator:

(1) Knowledge of latitude

    (a) Polar

    (b) Equatorial

    (c) Temperature

(2) Knowledge of temporal information

    (a) Seasonal

    (b) Diurnal

    (c) Sunspot cycle

(3) Real time information

    (a) Recognition of spurious effects

    (b) Rejection versus compensation and use

c. Ionospheric Error Analysis

For short ranges (R < 50 km), a flat-earth approximation is acceptable for most applications. However, as a check the greater part of the analysis summarized in this section was carried out for a spherical earth. Comparison with results for a flat earth indicated that use of the approximation was valid.

In Figure 6 the variation of zenith angle (θ) with range (R) is shown for two virtual heights and two modes, one and two hop per layer. Note that the zenith angle as used here is ($90° - \beta$) where β is the launch angle. To represent the F_2 layer, a virtual height of 300 km is assumed and for the E layer, 100 km. This graph gives the variation of zenith angle with distance for ranges in the area of $8 \leq R \leq 50$ km.

Since current information on the state of the ionosphere is essential, the final system considers the availability of an on-line ionosonde. This is necessary in order to determine the virtual height corresponding to the equivalent vertical incidence frequency (f_v). (f_v is found from the operating frequency by the "secant i law" where i is the angle of incidence of the ray upon the layer.)

16
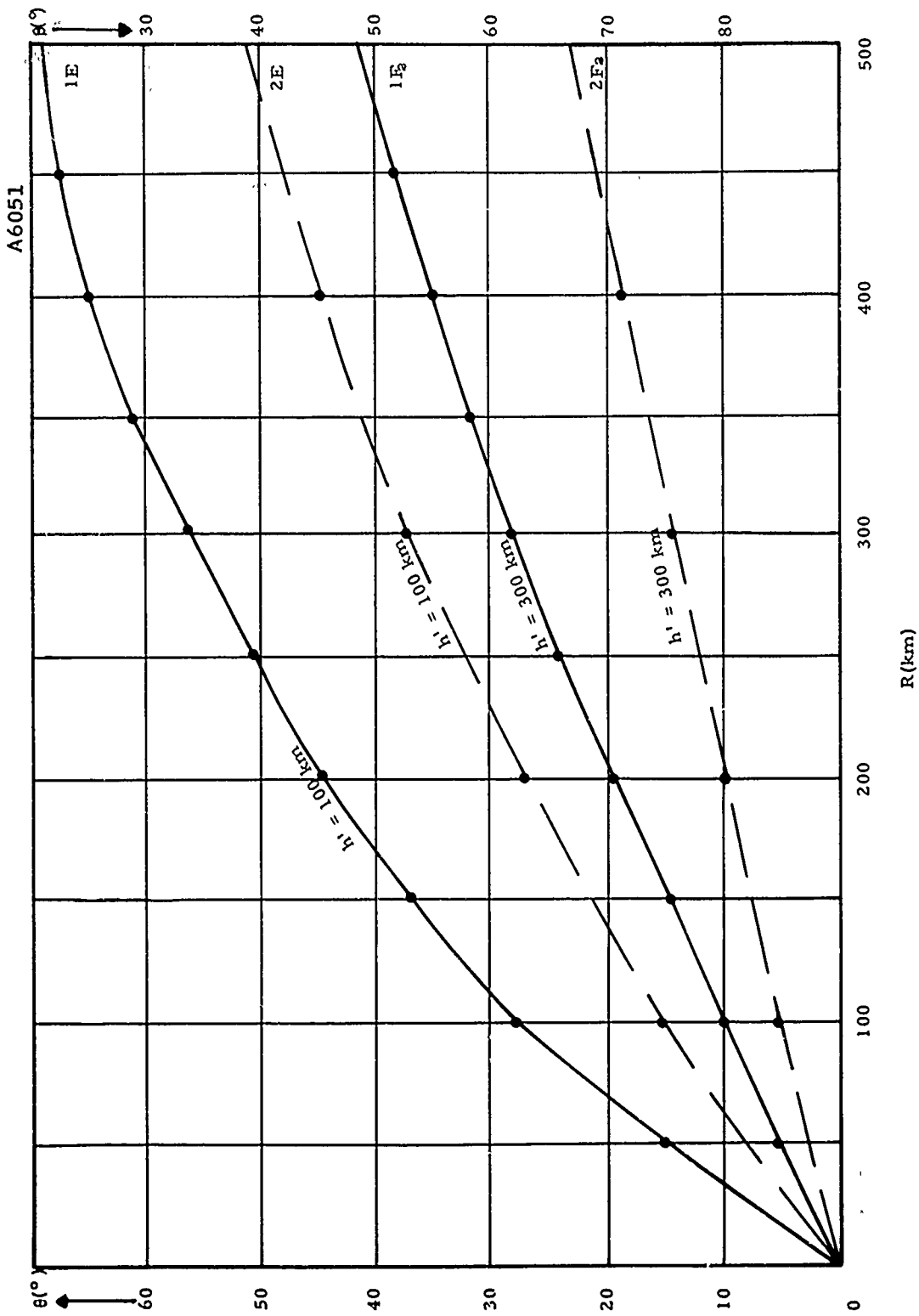
FIGURE 6 Zenith Angle (θ) and Elevation Angle (β) versus Distance Between Stations (R) for Various Virtual Heights (h') (U)

17

For planning purposes characteristics at the path reflection
point are frequently obtained from the ionospheric predictions.
While these serve a useful purpose, it must be recalled that
they represent the general climatology of the ionosphere for
the location and time considered. It is far superior to employ
current knowledge of the state of the ionosphere at the path
midpoint. In a practical situation, these observations may be
difficult to attain. However, it usually is possible to make
vertical incidence observation on a noninterfering basis at the
station site. The problem then becomes one of extrapolating
the data from overhead to the reflection point. On a general
basis the greater the distance the poorer the extrapolation.
Since the E and F_1 layers so closely follow the behavior in-
dicated by the ideal Chapman layer[4], their characteristics may
be projected with fair accuracy to considerable distances. Un-
fortunately the F_2 layer is not so well behaved and it becomes
difficult to define an accurate extrapolation function. Practice
has shown, however, that the vertical incidence soundings
made at one point hold fairly well to distances of about 150 km
without too much error while the error will increase with
increasing distance from the measuring point.

Note that the present study is concerned with ranges of the
order of $80 \leq R \leq 500$ km implying to a first approximation
that reflection points occur between 40 to 250 km from the
site. For these distances information supplied by an ionosonde
located at the site should not differ too much from that at the
reflection point and should therefore offer considerable im-
provement over the predictions. For these distances the
sounder data may be employed directly, or simple correc-
tions for distance may be introduced.

Figure 7 shows the effect of ionospheric tilts in producing
errors in range (δR). Let α = tilt of the layer downward to
the receiver with respect to the great circle between the two
sites. From Figure 7

$$\theta_2 = \theta_1 + 2\alpha \text{ for ionospheric tilt case.}$$

----

[4] Davies, Kenneth, "Ionospheric Radio Propagation", National
Bureau of Standards, pg. 18.

18

A6052
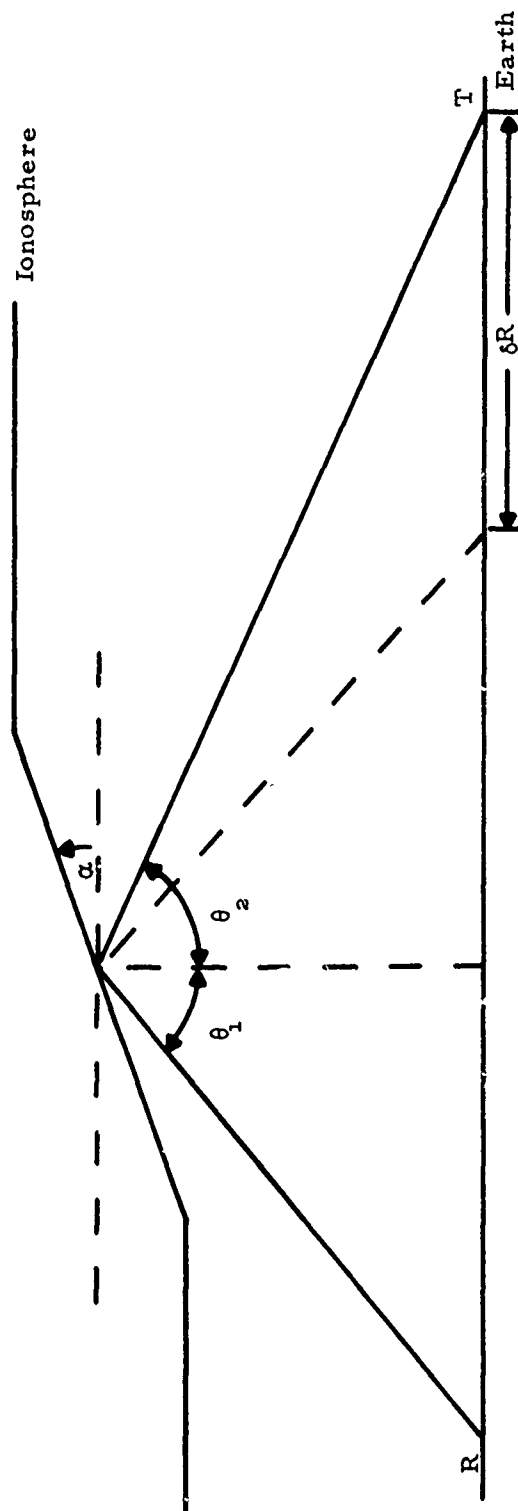
FIGURE 7 Distortion of Ray Path Due to Tilt (U)

19

Then

$$\delta R = h(\tan(\theta_1 + 2\alpha) - \tan\theta_1) \quad \text{(flat earth)}$$

The range, R, varies as a function of virtual height, h; zenith angle, θ; and tilt angle, α, as follows:

$$R = h\tan\theta + h\tan(1 + 2\alpha) \quad \text{(flat earth)}$$

$$R = a_0\pi + a_0\theta - 2a_0\alpha - a_0\sin^{-i}\left[\sin(\theta + 2\alpha)\right.$$

$$\left. + \frac{\sin(\theta - \sin^{-1} t)\sin 2\alpha}{t}\right] - 2\alpha\sin^{-1} t \quad \text{(curved earth)}$$

where

$$a_0 = \text{radius of earth} = (6370 \text{ km})$$

$$t = \frac{a}{a+h}\sin\theta$$

The curved-earth equation was used in constructing the curves of Figure 8. In Figure 8 resulting errors in range $\left|\frac{\delta R}{R}\right| \times 100\%$ due to various tilt angles (α) are shown. Computations were carried out with spherical earth approximations, and representative heights of 100 and 300 kms were used as additional parameters. Although curves for only positive tilt angles ($\alpha = 0.5°$, $1°$, $2°$) are plotted, negative tilt angles were found to have almost identical corresponding curves; e.g., the range error for these short distances due to $\alpha = -1°$ is nearly the same as that corresponding to $\alpha = 1°$.

Under the criterion of a tolerable error in range of 10 per cent, only the combined conditions of short range and high heights appear worthy of our concern.

Bramley and Ross[5] have shown that typical tilt (rms) for the F layer vary from $\pm 1°$ to $\pm 2°$ and are even less for the E layer. Their durations may vary from minutes to hours with

----

[5]

Bramley, E. N., Ross, W., "Measurement of the Direction of Arrival of Short Radio Waves Reflected at the Ionosphere", Proceedings of the Royal Society, A, 220, 1951.

20
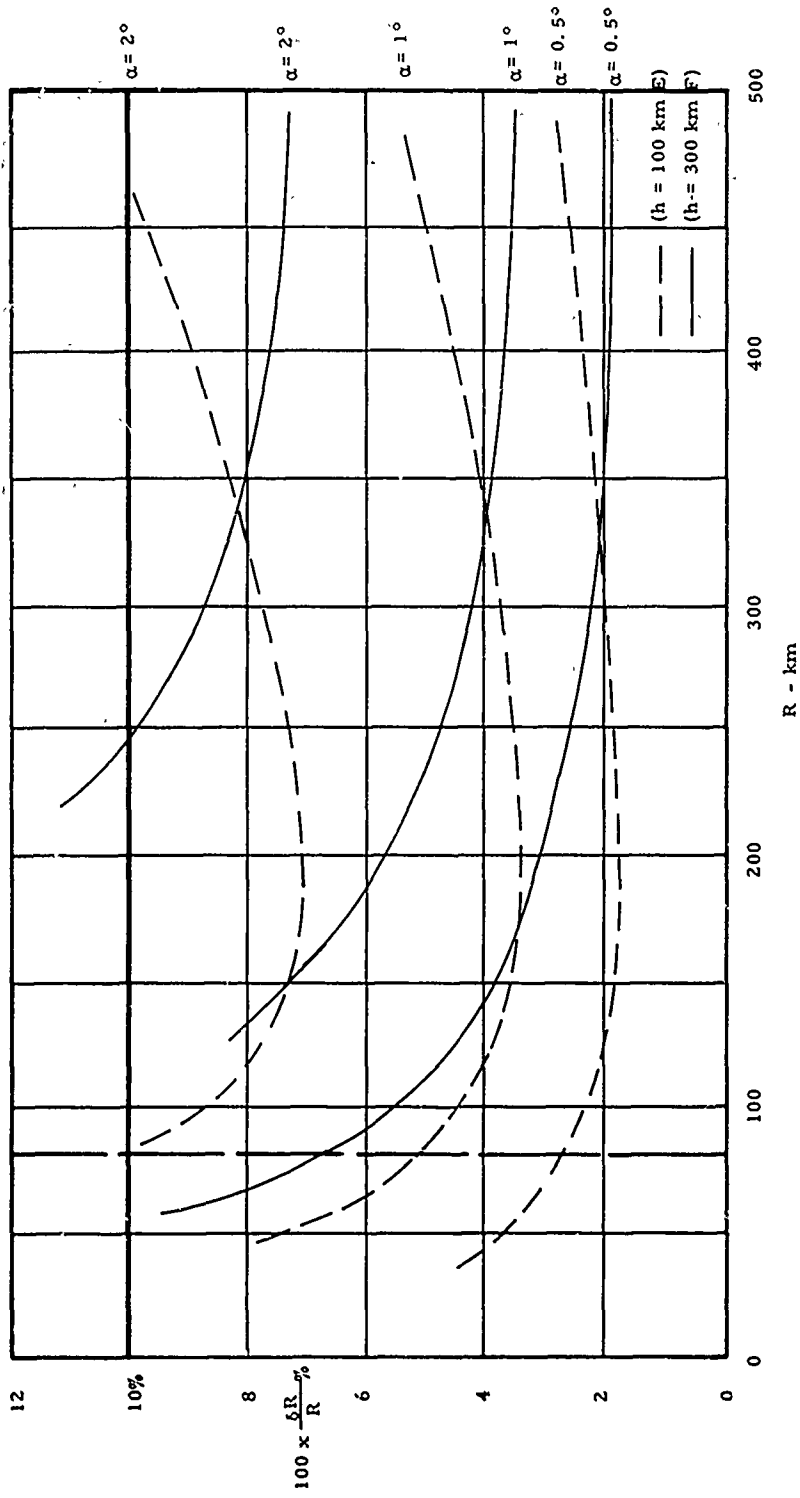
FIGURE 8 Per Cent Error in Range Due to Tilt versus
Range for Various Tilt Angles (U)

B6053

21

perhaps a mean of 5 to 30 minutes. They arise from the undulating structure and movements of the layers.

Another consideration is that of Sporadic $E(E_s)$. E_s is a heavily ionized layer near the normal E layer in height. It appears in scattered, isolated instances which makes prediction, with any degree of accuracy, considerably difficult.

Reflection from Sporadic E may "blanket" or prevent reflection from the normal F_2 layer. This blanketing effect extends up to the equivalent vertical incidence blanketing frequency of E_s. Under conditions where blanketing E_s occurs, azimuthal accuracies for one-hop propagation may exceed those obtained from any other mode. This statement, however, neglects possible tilts of the E_s layer[6,7] and the possibility of edge or side reflection from the E_s cloud. Also, the presence of E_s may introduce other complications. If a localized cloud of limited extent is present, complex modes (e. g., M, N, etc.) may appear making a determination of range from a knowledge of the vertical arrival angle difficult. Note that when the ranges are relatively small ameliorating factors appear. For ranges less than about 500 km, the probability is fairly high that only single or double-hop reflection can occur. Measured launch angles when double hop is present always exceed those for single hop (see Figure 6).

It is possible to recognize the presence of double hop E_s propagation fairly well at least during the summer months. At this time, in the northern hemisphere

(1) values of f_o F_2 are relatively low and

(2) values of f_o E_s are relatively high.

Also, Sporadic E occurs with greatest frequency during the period 0800-2000 LST. If during this period high vertical angle

6 ------------
  Harris, R. D., Jensen, D. R., Clark, C., "Analysis of Backscatter Studies", Final Report, Utah State University, Logan 1965.

7
  Gerson, N. C.,. Geddes, W. H., "Propagation Data Analysis", Second Quarterly Progress Report, 1 October 1966 through 30 December 1966, Contract DA18-119-AMC-01952(X), Task No. 14, Electronics Research Laboratory, Syracuse University Research Corporation, Syracuse, New York, 27 February 1967.

reception is noted, it would appear probably that double hop E_s propagation had occurred. While this assumption is probably valid in the great percentage of cases, information from an on-line vertical ionosonde would greatly assist in defining the modes involved.

Also, due to these characteristics of E_s during the summer months and because the ranges under consideration are relatively short (< 500 km), a receiving operator can be fairly well assured that if an oblique signal is received and an E_s layer is determined to be directly overhead then the incoming wave is traveling only via the E_s layer and not by either the F_2 layer or a combination of both F_2 and E_s (N-type mode). This conclusion is arrived at by recognizing that the short ranges of operation require for F_2 propagation large elevation angles (or small zenith angles (Figure 7)), and so the low F_2 critical frequency approximates the MUF of the F_2 layer. Hence, as long as the operating frequency is not too low, an absence of F_2 layer propagation can usually be assumed. This requires any propagation to be via the E_s layer.

A quick check can be performed to determine with good probability from which layer (E_s or F_2) the signal is reflecting. If the operating frequency f satisfies

$$f < f_0 \, E_s \, \sec i_s$$

where $f_0 \, E_s$ is the vertical incidence critical frequency of the Sporadic E layer and i_s is the apparent angle of incidence that the ray makes at this layer (if it reflects from it), then the E_s and not the F_2 is most likely the layer used for propagation. The angle i_s can be approximated from geometric considerations by the relation

$$\frac{\sin i_s}{a_0} = \frac{\cos \beta}{h'_s + a_0}$$

where

a_0 = radius of earth

h'_s = virtual height of E_s (may be approximated to 100 km)

β = angle of arrival

23

An on-line computer may be available to facilitate the computation.

d.   <u>In Situ Tilt Check</u>

Checking for tilt conditions can be made by making known station comparisons for a reliability assessment. Another technique is to look for time variations in range (especially day/night) for reliability assessment and correction.

e.   <u>Ionosonde Prediction Studies Procedure</u>

A comprehensive study has recently been completed demonstrating which modes of operation can be expected and the relative power loss between them. Only the common modes were considered: one and two hop E and F_2 reflections (see Figure 9). The parameters considered were diurnal variation (hourly), seasonal variation (represented by the months December, March, June and September), geographical location (arctic, temperate, and tropic), operating frequencies (2 - 12 MHz), and transmitter to receiver ranges of 50, 250, and 500 km. The year 1967 was chosen as a model year for acquiring data on which to base the computations. This is primarily because this was the most recent year of which an entire set of ITSA f_0 F_2 and M(3000) F_2 factor prediction data cards were available. The average sunspot number (12-month moving average as observed at Zurich, Switzerland) for the year 1967 was 96.

The procedures used for determining the occurrence of various modes of propagation are basically variations of the procedures outlined in ITSA-1[3].

In the employ of the ITSA-1 prediction technique, the following assumptions were utilized:

(1)   Lower level refraction was ignored.

(2)   Shimazoki's formula[8] for computing the maximum ionization height of the F_2 layer was assumed adequate.

----

[8] Shimazoki, F., "World-Wide Daily Variations in the Height of the Maximum Electron Density of the Ionospheric F_2 Layer", J. Radio Res. Labs, 2, No. 7, Japan, January 1955.

COMMON MODES
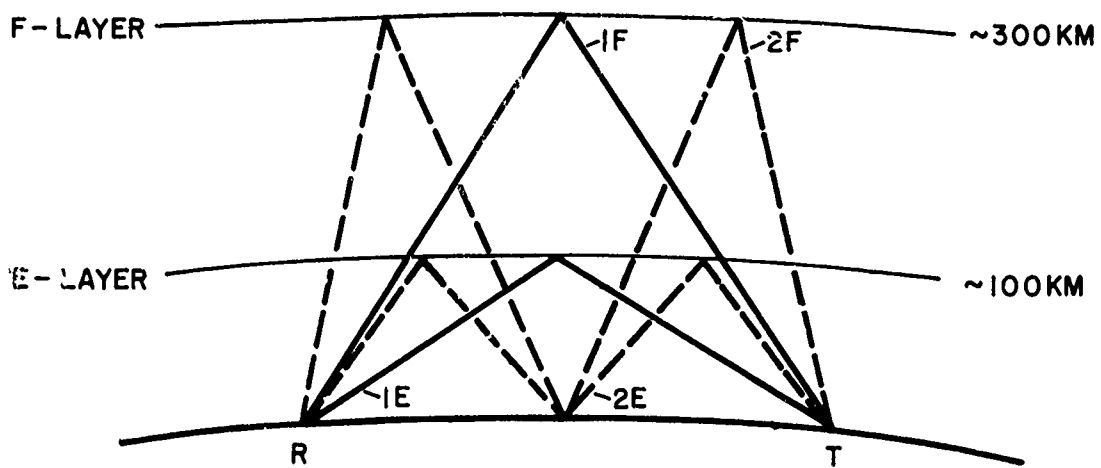
FIGURE 9   Common Ray Paths via the Ionosphere for
Short Transmitter to Receiver Distances (U)

25

(3) Parabolic layer theory was used throughout.

f. Results

Figures 10 through 15 show the results of the predictive model study. It is noted that usually only two modes are effective within 500 km. Equally important is the fact that the stronger mode, usually the 1F, exceeds the others by 10 dB in most cases (see Table 2). This latter fact will be used to advantage in the signal processing which is described herein.

g. Conclusions

The results of this study indicate the following conclusions should be made:

(1) Ionosphere well-behaved

(2) Anomalies detectable, sometimes correctable

(3) Normally two rays present

(4) One ray generally stronger by 10 dB to 30 dB

(5) For 80 km ≤ R ≤ 500 km, zenith angles (θ) are < 45 degrees

3. WAVE INTERFERENCE (U)

The following discussion uses the system of coordinates shown in Figure 16 and the symbols have meaning as defined in the appendix. Figure 17 shows the mathematical expression for two elliptically polarized plane waves, $\vec{A}(t)$ and $\vec{B}(t)$, traveling in directions $\vec{k}_1$ and $\vec{k}_2$, respectively, with a time phase difference $\beta(t)$:

$$\vec{A}(t) = \mathrm{Re}\left[\left(A_\theta \vec{u}_{\theta_1} + A_\Phi\, e^{j\delta_1}\, \vec{u}_{\Phi_1}\right) e^{j(\omega t - \vec{k}_1 \cdot \vec{r})}\right] \qquad (1)$$

$$\vec{B}(t) = \mathrm{Re}\left[\left(B_\theta \vec{u}_{\theta_2} + B_\Phi\, e^{j\delta_2}\, \vec{u}_{\Phi_2}\right) e^{j(\omega t - \vec{k}_2 \cdot \vec{r} + \beta(t))}\right] \quad (2)$$

As shown in Figure 16, consider a pair of antennas parallel to the x-axis and located at (x = 0, y = a, z = 0) and (x = 0, y = -a, z = 0), respectively. The complex voltages, V_a and V_b, induced in the antennas are:

26
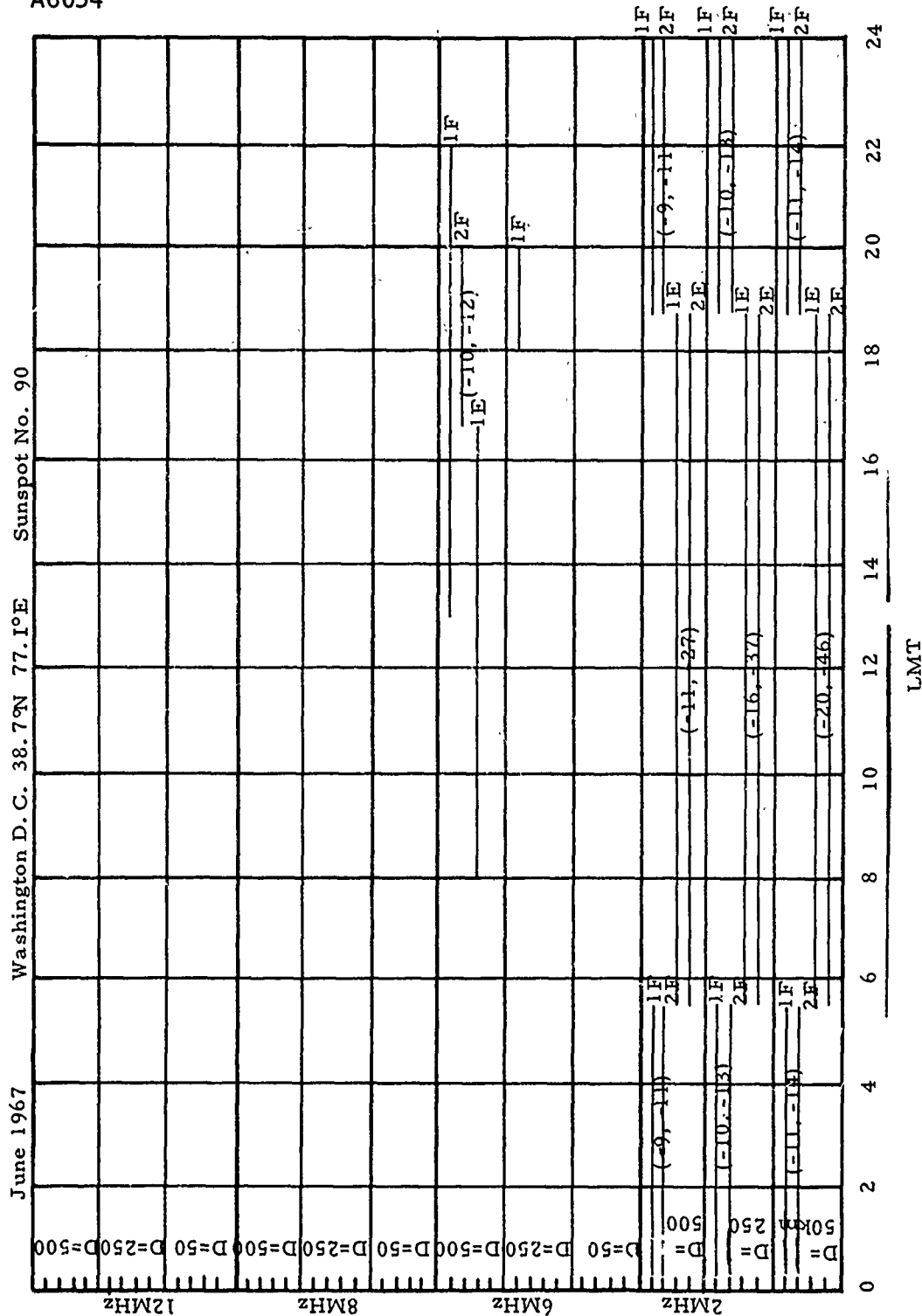
FIGURE 10 Expected Sky-Wave Modes for Washington, D. C.; in June 1967 Showing Attenuation in dB with Respect to Stronger Mode (U)

27
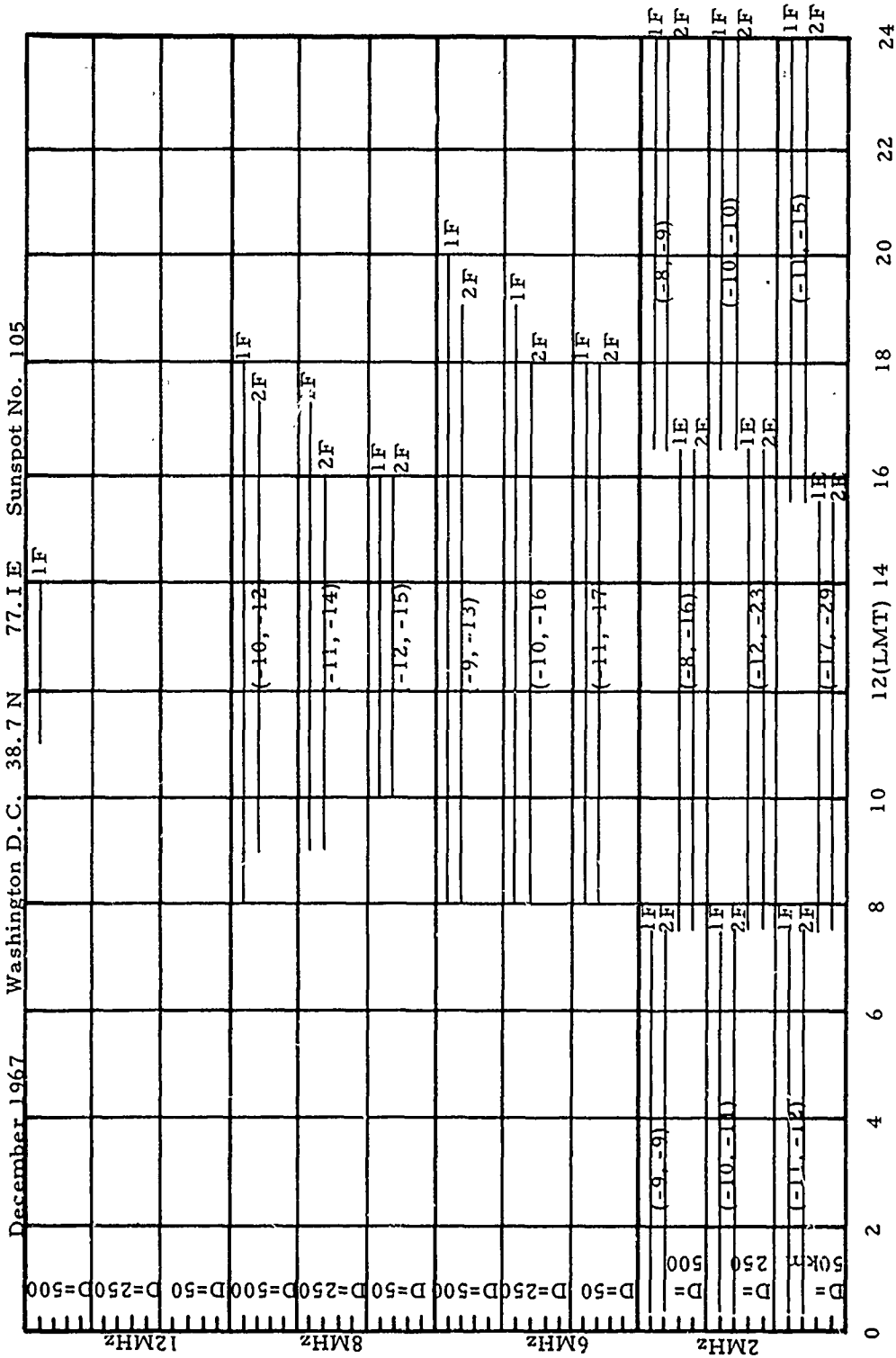
FIGURE 11 Expected Sky-Wave Modes for Washington, D. C., in December 1967 Showing Attenuation in dB with Respect to Stronger Mode (U)

28

A6056

FIGURE 12 Expected Sky-Wave Modes for Saigon in June 1967
Showing Attenuation in dB with Respect to Stronger
Mode (U)

29
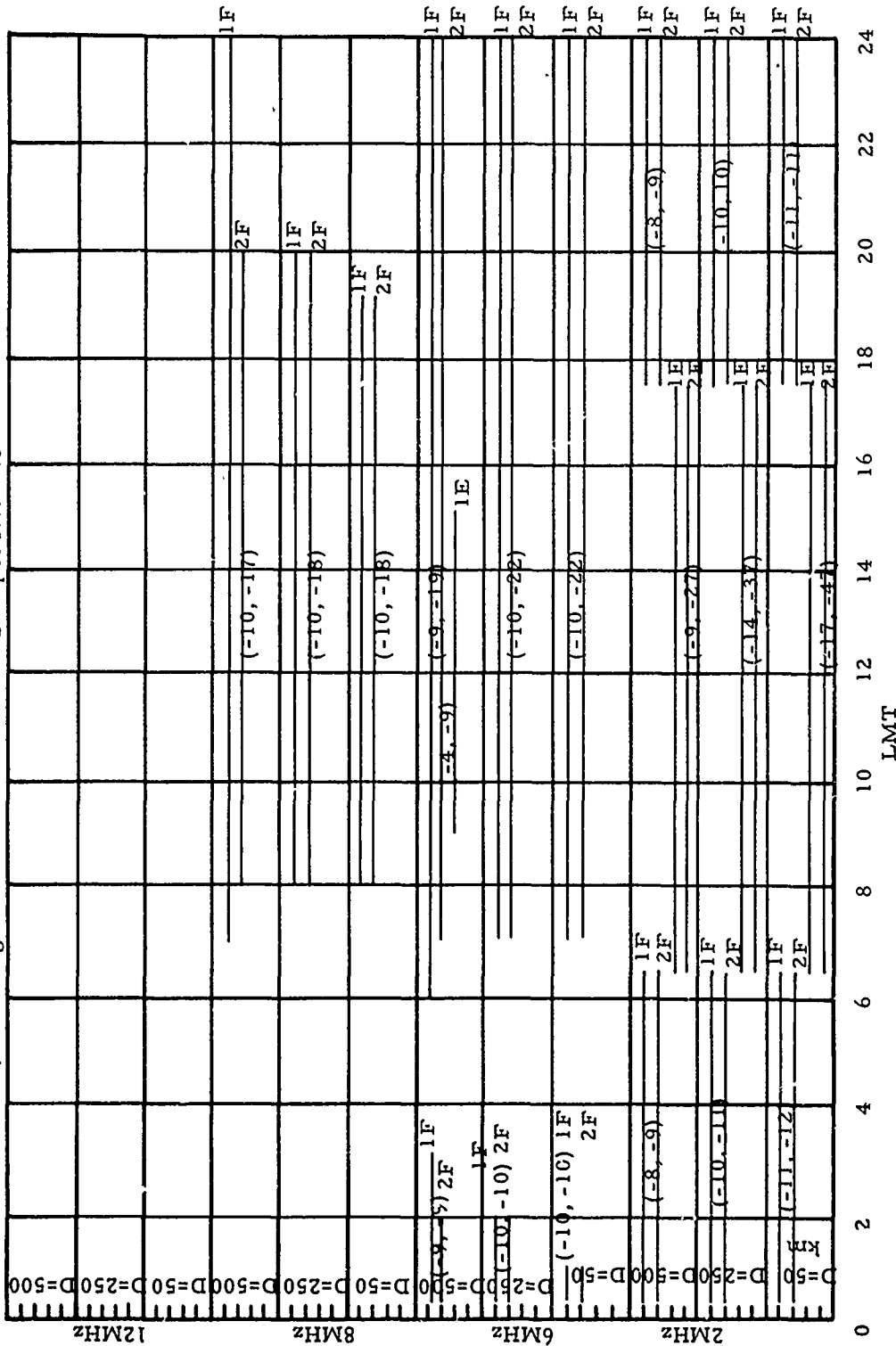
FIGURE 13 Expected Sky-Wave Modes for Saigon in December 1967 Showing Attenuation in dB with Respect to Stronger Mode (U)

30

A6058
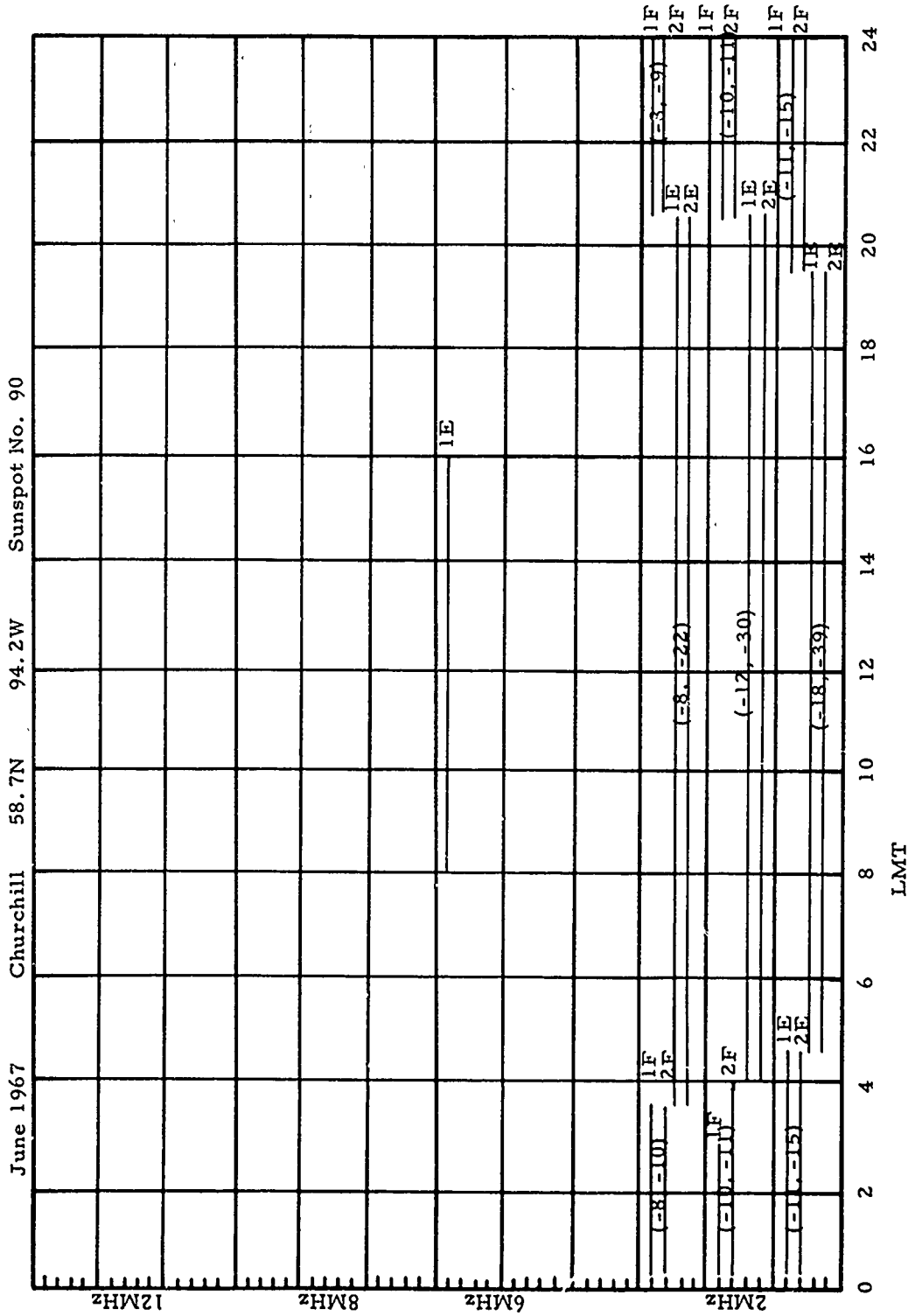
FIGURE 14 Expected Sky-Wave Modes for Churchill in December 1967 Showing Attenuation in dB with Respect to Stronger Mode (U)
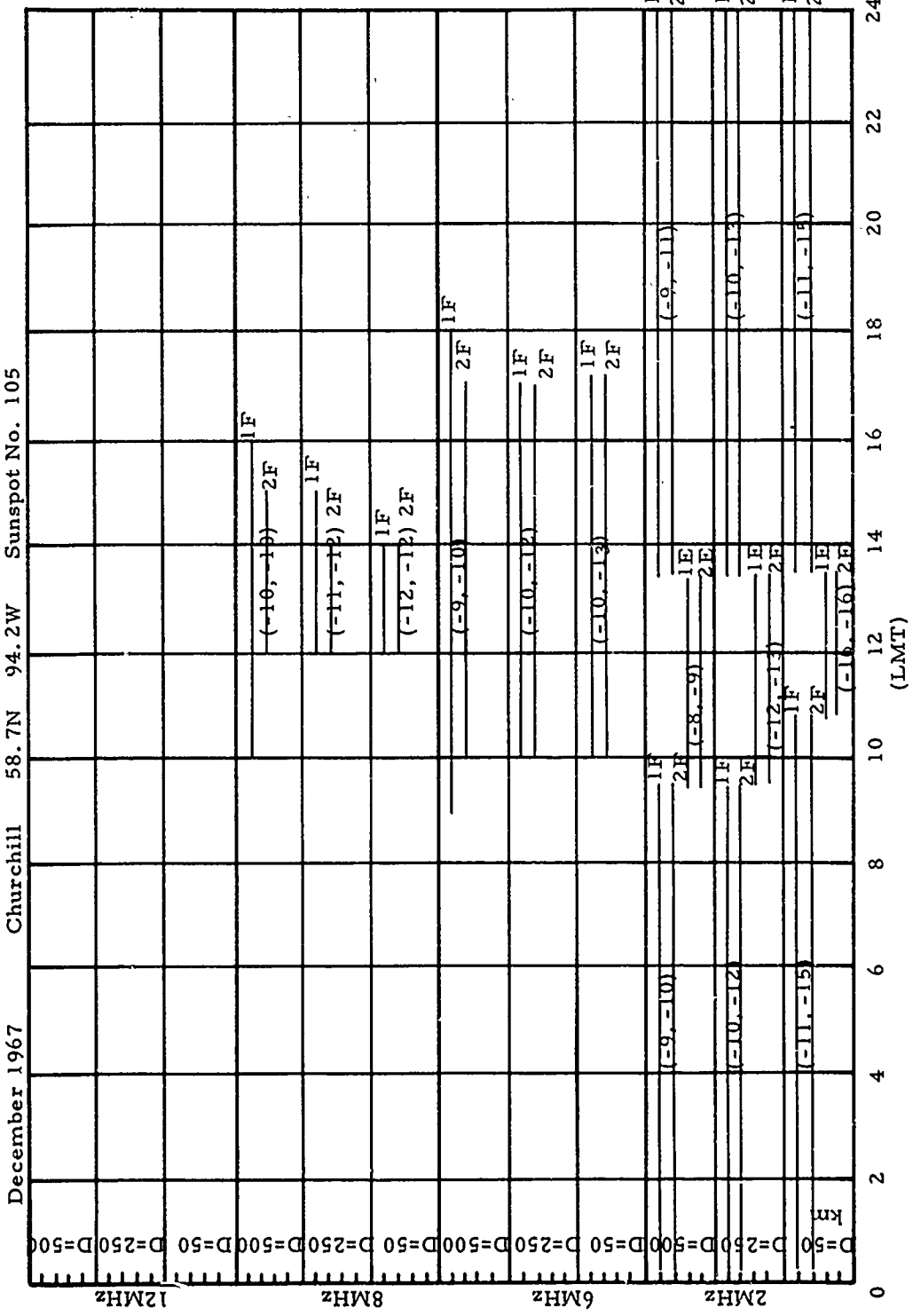
FIGURE 15 Expected Sky-Wave Modes for Churchill in December 1967 Showing Attenuation in dB with Respect to Stronger Mode (U)

A6059

32

TABLE 2 Results from Sky-Wave Prediction Study Emphasizing Ionospheric Propagation Expectation

Geographic Latitude	Magnetic Latitude	Place	One or Two Rays Present (Given a Ray Occurs)	One or Two Rays With More Than 10 dB Difference (Given a Ray Occurs)
58.7	68.0	Churchill	99%	80%
38.7	50.0	Washington	97%	82%
10.5	3.5	Saigon	95%	73%

R = 50, 250, 500 km

F = 2, 6, 8, 12 MHz

Seasonal variation represented by March, December, June, and September

Mean sunspot number = 97

33
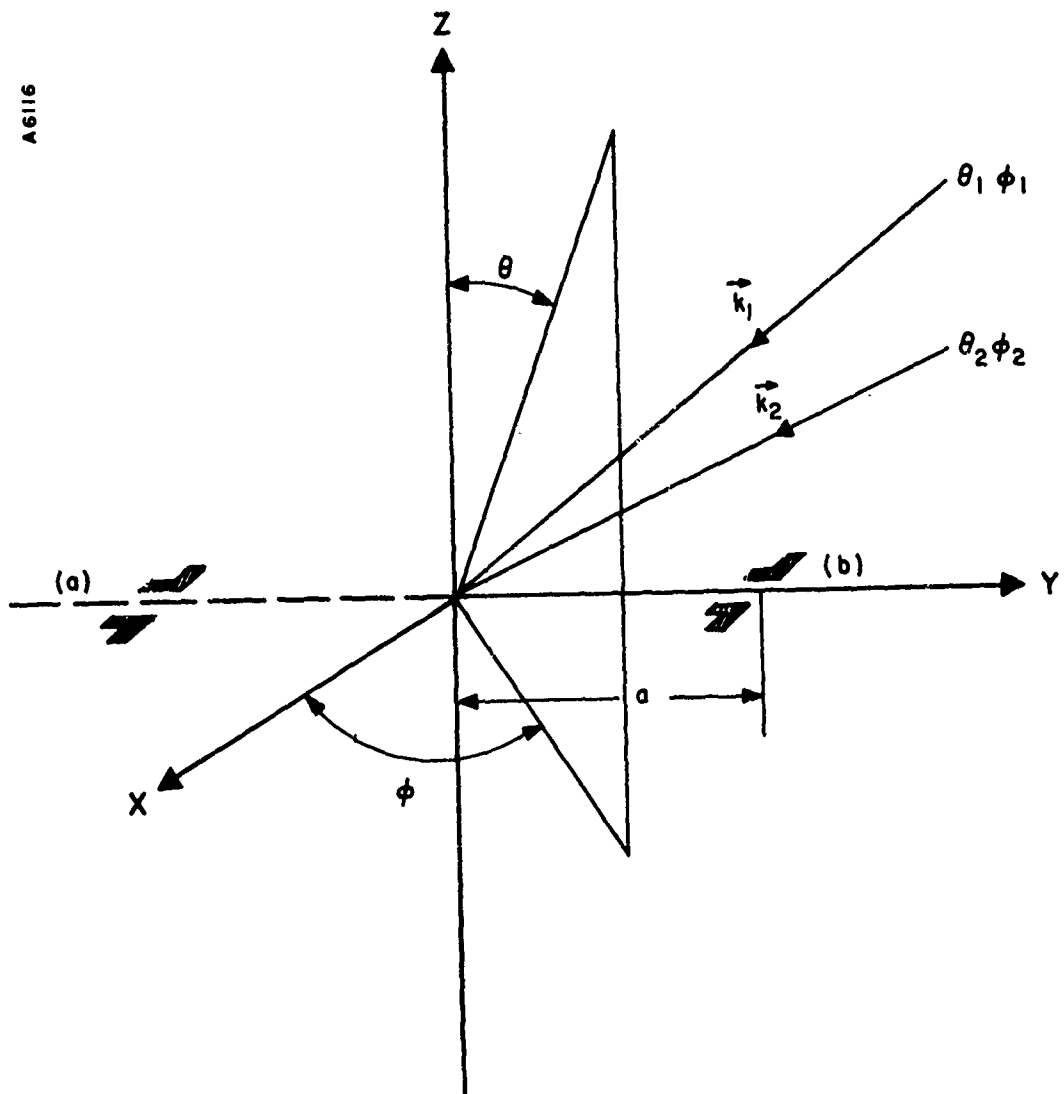
FIGURE 16 Coordinate System Including Antenna Elements (U)

A6116

34

$$V_a \sim A(\delta_1) e^{j\psi_1} + B(\delta_2) e^{j(f(\delta_2) - f(\delta_1) + \beta)} e^{j\psi_2}$$

$$V_b \sim A(\delta_1) e^{-j\psi_1} + B(\delta_2) e^{j(f(\delta_2) - f(\delta_1) + \beta)} e^{-j\psi_2}$$

The net result may be interpreted as follows: The amplitude variation of $A(\delta_1)$ is strongly dependent on the time phase δ_1 between the two orthogonal components A_θ, A_ϕ, of the vector $\vec{A}$. A similar remark holds for $B(\delta_2)$. The variations occur not because of the polarization of the wave but because of the changes in the polarization. The phase variation of either V_a or V_b is also strongly sensitive to changes in δ_1 or δ_2.

Mathematical Description: $A(t) + B(t)$

Where

$$A(t) = Re(A_\theta \underline{u}_\theta + A_\phi e^{j\delta_1(t)} \underline{u}_\phi) e^{j(\omega t - \vec{k}_1 \cdot \vec{r})}$$

$$B(t) = Re[(B_\theta \underline{u}_\theta + B_\phi e^{j\delta_2(t)} \underline{u}_\phi) e^{j\beta(t)}] e^{j(\omega t - \vec{k}_2 \cdot \vec{r})}$$

Polarization: In general, elliptical

Direction: $\vec{k}_1$, $\vec{k}_2$

Phase Difference: $\beta(t)$

FIGURE 17 Wave Interference (U)

Figure 18 shows a phasor representation of the antenna voltages V_a and V_b. This figure illustrates how the magnitudes of V_a and V_b, as well as their relative phase difference γ, depend on the magnitudes and phases of the interfering waves: $A(\delta_1)$, $B(\delta_2)$, $\beta'(t)$.

As $\beta'(t)$ varies randomly, the probability distribution of the angle that V_a makes with the real axis is symmetrical with respect to ψ_1. Therefore, this angle, averaged over many random values of $\beta'(t)$ is ψ_1. A similar argument holds for V_b. The total average phase difference, $\overline{\gamma}$, between V_a and V_b is therefore equal to $2\psi_1$.
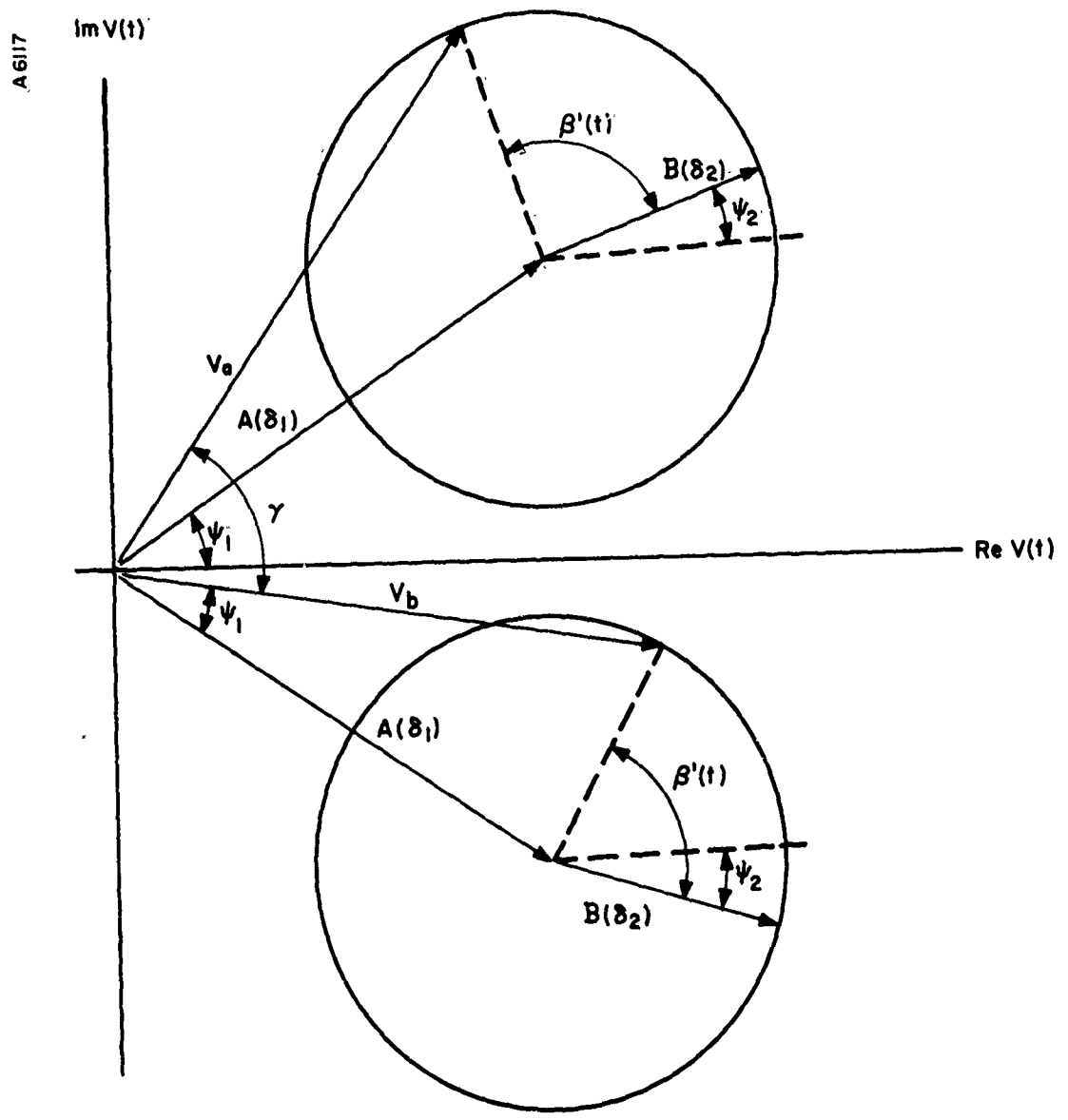
FIGURE 18   Phasor Diagram (U)

36

This last statement may be expressed mathematically by the theorem that follows. The theorem holds for all the distributions $\beta'(t)$ that allow an integration with respect to time to be replaced by an integration with respect to β.

Theorem:

Let

$$E_1 = Ae^{j\psi_1} + Be^{j(\psi_2 + \beta)} = |E_1| e^{j\gamma_1}$$

$$E_2 = Ae^{-j\psi_1} + Be^{-j(\psi_2 - \beta)} = |E_2| e^{j\gamma_2}$$

then

$$\overline{\gamma_1 - \gamma_2} = 2\psi_1$$

If A and B are time varying but $|A| < |B|$ at every instant of time, then the branch point never moves inside the contour; hence under these conditions the theorem still holds. From this we may conclude that the following corollaries are true.

Corollary I

> If A and B are time varying but $|A(t)| > |B(t)|$ consistently, $\gamma \to 2\psi_1$ as the sampling time increases.

Corollary II

> If A > B some of the time
> and B > A the rest of the time
> but $|\overline{A}| > |\overline{B}|$, the average phase $\overline{\gamma}$ lies between
> $2\psi_1$ and $(\psi_1 + \psi_2)$.

Verified by computer experiments and proven analytically.

4. PROBABILITY DISTRIBUTION OF THE PHASE DIFFERENCE AT THE ANTENNA TERMINALS (U)

Computer analysis furnished information as to the probability distribution of γ as $\beta(t)$ was allowed to vary randomly. Two main cases are of interest, but for all cases $\beta(t)$ assumes an independently random variation.

Case I: A and B maintained constant
            A = 10, B = 1, 3, 5, 8, 10

Case II: A and B vary randomly with limits
            $0 \leq A \leq 10; 0 \leq B \leq 1, 3, 5, 8, 10$

Case IIA: Same as Case II; however, two distributions
            are obtained:

            a. $A \geq B$

            b. $B \geq A$

In the first case, 2,000 random values of β yielded a probability
distribution similar to that shown in Figure 19 for all values of B.
Figure 20 represents the case A = 10, B = 5. Two conclusions
can be drawn from this portion of the study. For each distribution
the average is $2\psi_1$, that phase associated with the stronger ray. It
is also noted that the most probable phase does not correspond to
either of the two directions of arrival. Thus under the condition of
two mode propagation, with stable amplitudes, the phase indicated
most often is in error with respect to both rays.

The second case considered 3,000 random independent samples of
A, B, and β. The probability distribution shown in Figure 21
illustrates $0 \leq A \leq 10; 0 \leq B \leq 5$. There are two local peaks in
the curve as well as a main peak. The main peak corresponds to
$2\psi_1$, while the other two correspond, one to the average phase of
the distribution, the other to $2\psi_2$, the phase associated with the
weaker ray, B. It is noted that the average phase no longer cor-
responds to $2\psi_1$, but is a function of the upper limits set on B.
This error is shown in Figure 22. The error is zero in the limiting
case of a vanishing weaker ray and reaches a maximum of

$$\frac{\psi_1 - \psi_2}{2}$$

when the upper limits of A and B become equal.

The final case is but an alteration of Case II. For each calculation
of γ, the computer distinguished whether A was greater than B
and vice versa. In this way, two probability distributions were
constructed, the sum of which is represented by the previous case.
Figure 21 shows the distribution in red for B > A and in black for

38

A 6119

A=10.0
B= 5.0
$2\psi_1 = 24.34°$
$2\psi_2 = 12.97°$
SAMPLES: 2000
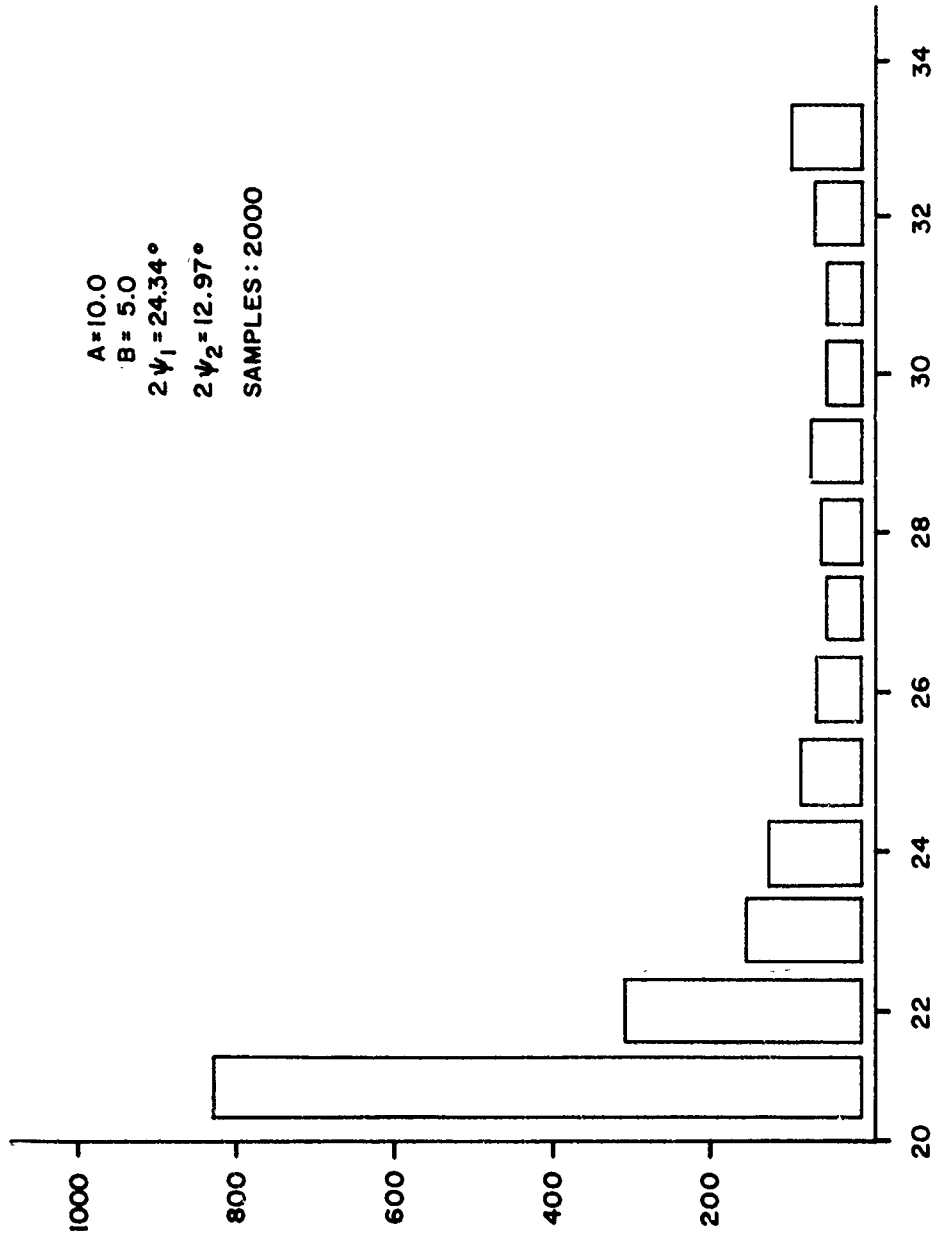
FIGURE 19 Probability Distribution (U)

39
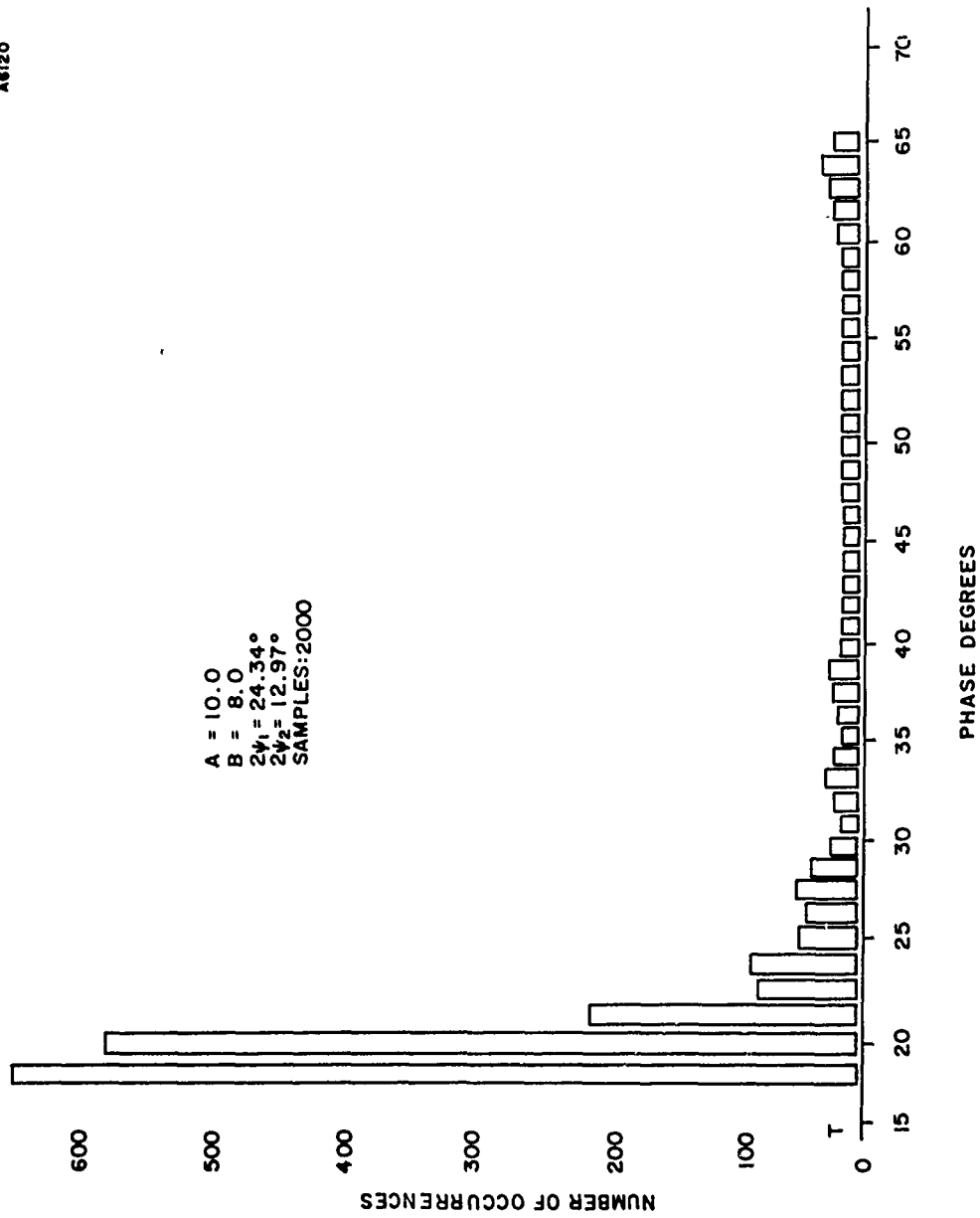
FIGURE 20 Probability Distribution (U)

40
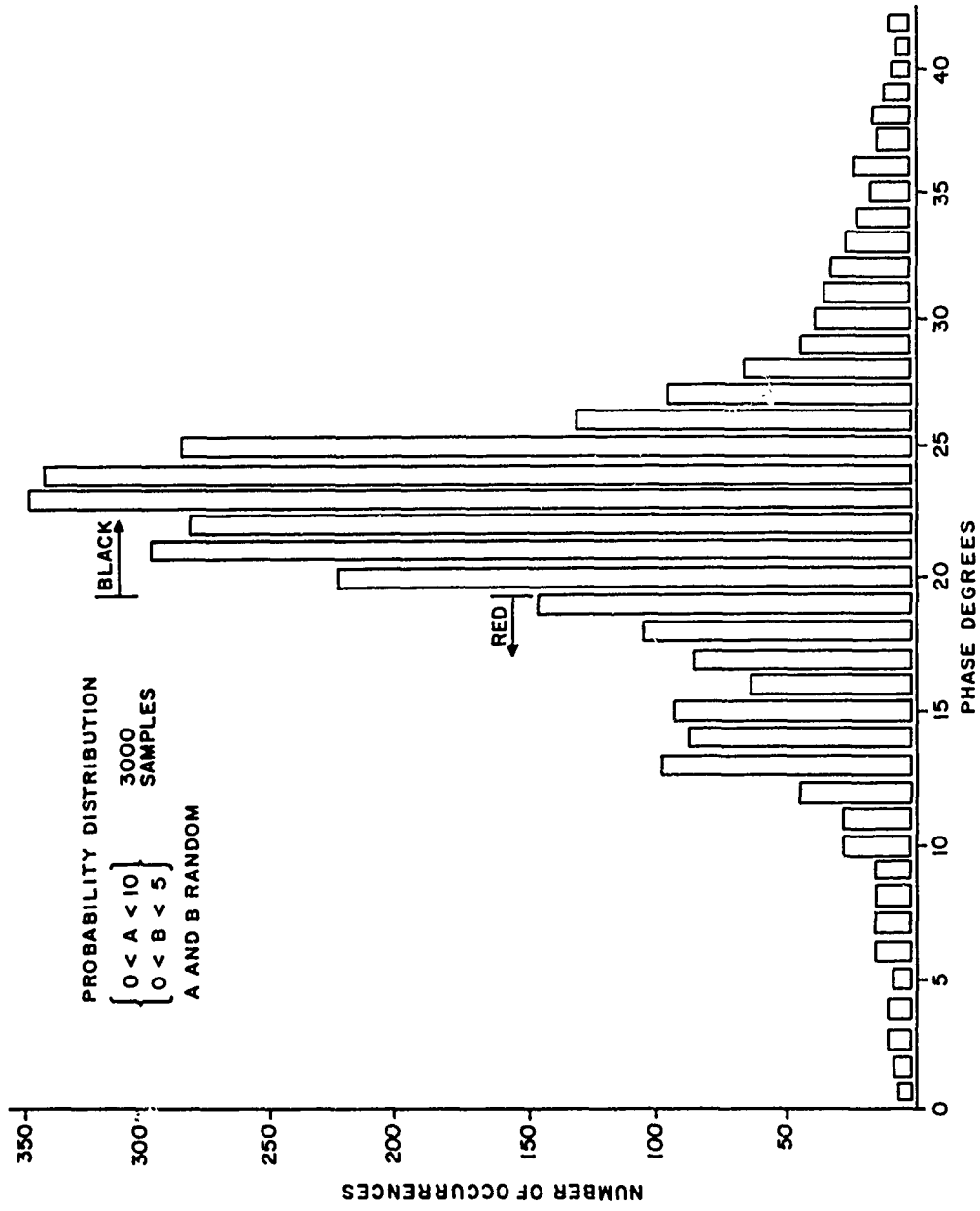
FIGURE 21 Probability Distribution (U)

PROBABILITY DISTRIBUTION

$\left.\begin{array}{l} 0 < A < 10 \\ 0 < B < 5 \end{array}\right\}$

3000 SAMPLES

A AND B RANDOM

BLACK

RED

NUMBER OF OCCURRENCES

PHASE DEGREES

41

A6118
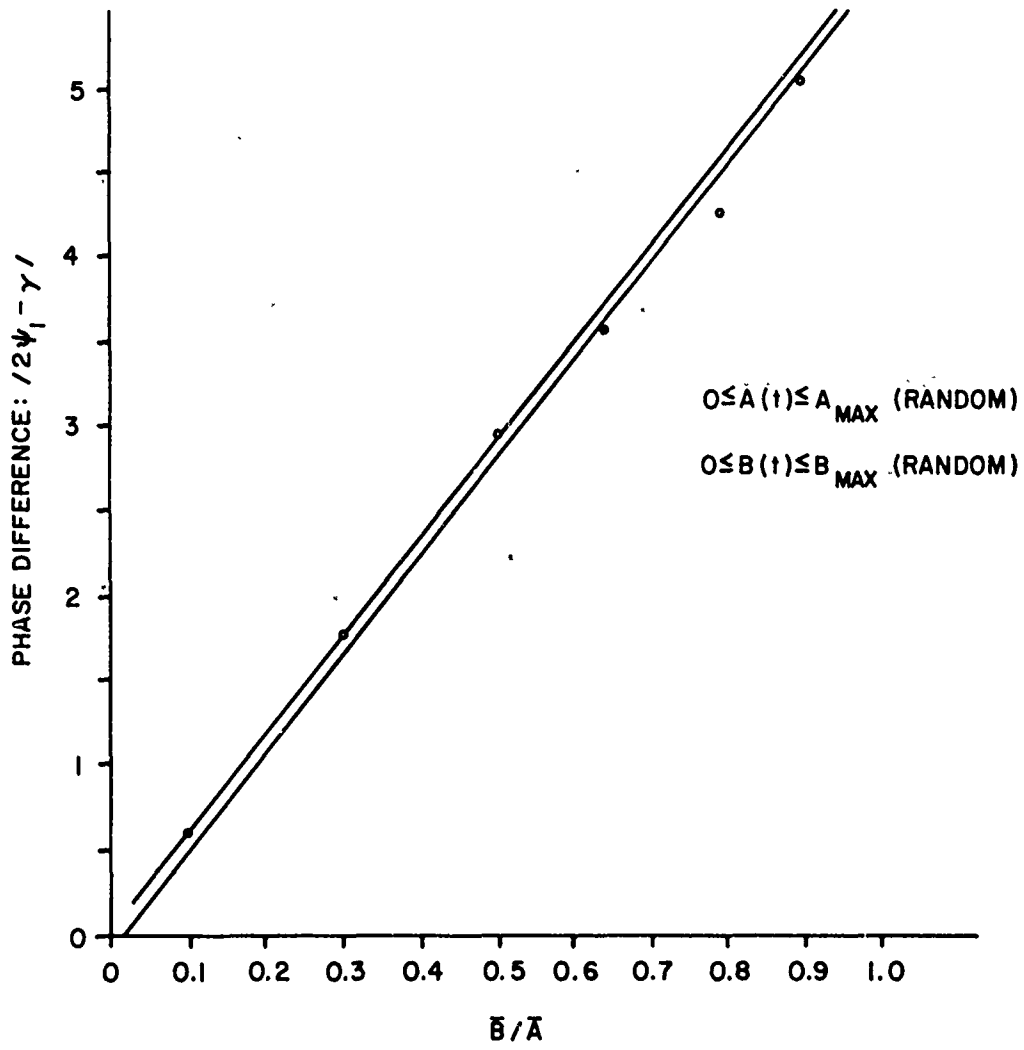
FIGURE 22   Difference between Average Phase and $2\psi_1$ (U)

A > B. Notice that the histograms do not overlap except for $\gamma = 19$ where rounding off of the phases to the nearest degree caused a slight ambiguity. For these two distributions, the averages are $2\psi_1$ and $2\psi_2$, respectively. From these results one may reach two major conclusions:

(a) When one ray is stronger consistently but amplitudes are varying, averaging still yields the phase corresponding to the stronger ray.

(b) The second conclusion is that if one could differentiate as to which ray was stronger for a given example, then averaging over many samples could be performed to give the directions of arrival of each mode.

Further investigation of this possibility is necessary.

5.   EXPERIMENTAL RESULTS (U)

Basically, the system used for direction finding is a phase measuring device. To apply the time averaging theorem discussed in the previous chapter, the phase between the voltages induced in a pair of horizontal dipoles must be measured at successive intervals of time. The heart of the system is a 90-degree hybrid which is conveniently used to convert the problem of measuring phases into one of measuring voltages.

V_1 o———   ———o V_3

Input   90° Hybrid   Output

V_2 o———   ———o V_4
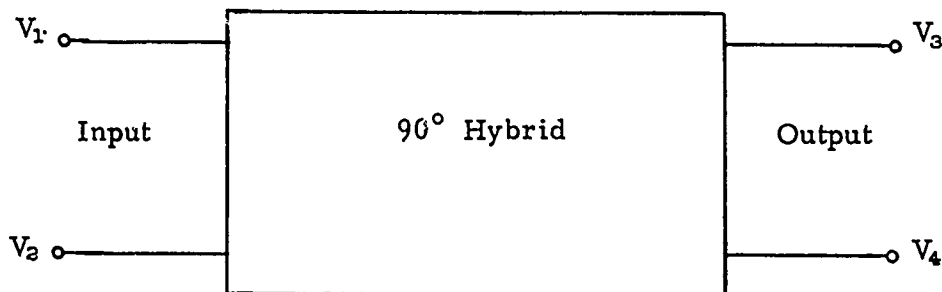
FIGURE 23   Voltage References for the 90-Degree
                    Hybrid (U)

43

This particular application of the hybrid was developed by Jules A. Cummins of the Syracuse University Research Corporation, and is given here. The voltage references are shown in Figure 23.

Let:

$$V_1 = |V_1| e^{j0} = |V_1| \tag{3}$$

$$V_2 = |V_2| e^{j\gamma} \tag{4}$$

Then if the hybrid is ideal, the voltages V_3 and V_4 are related to V_1 and V_2 by:

$$V_3 = \frac{|V_1|}{\sqrt{2}} (1 - jqe^{j\gamma}) \tag{5}$$

$$V_4 = \frac{|V_1|}{\sqrt{2}} (-j + qe^{j\gamma}) \tag{6}$$

where

$$q = \frac{|V_2|}{|V_1|} \tag{}$$

from which one obtains:

$$|V_3|^2 = \tfrac{1}{2} |V_1|^2 (1 + q^2 + 2q \sin \gamma) \tag{7}$$

$$|V_4|^2 = \tfrac{1}{2} |V_1|^2 (1 + q^2 - 2q \sin \gamma) \tag{8}$$

Adding:

$$|V_3|^2 + |V_4|^2 = |V_1|^2 (1 + q^2) = |V_1|^2 + |V_2|^2 \tag{9}$$

Subtracting:

$$|V_3|^2 - |V_4|^2 = 2 |V_1| |V_2| \sin \gamma \tag{10}$$

$$\sin \gamma = \frac{|V_3|^2 - |V_4|^2}{2 |V_1| |V_2|} \tag{11}$$

44

Subtracting $2\left|V_1\right|\left|V_2\right|$ from both sides of Equation 9:

$$\left|V_3\right|^2 + \left|V_4\right|^2 - 2\left|V_1\right|\left|V_2\right| = \left(\left|V_1\right| - \left|V_2\right|\right)^2$$

$$2\left|V_1\right|\left|V_2\right| = \left|V_3\right|^2 + \left|V_4\right|^2 - \left(\left|V_1\right| - \left|V_2\right|\right)^2 \tag{12}$$

Now Equation 11 can be written as:

$$\sin\gamma = \frac{\left|V_3\right|^2 - \left|V_4\right|^2}{\left|V_3\right|^2 + \left|V_4\right|^2 - \left(\left|V_1\right| - \left|V_2\right|\right)^2} \tag{13}$$

The determination of γ involves, therefore, three voltage measurements. The usual restriction of having $\left|V_1\right| = \left|V_2\right|$ for this type of phase meter can be thus removed by measuring the difference between the input voltages.

The entire data collection system is shown in Figure 24. To simplify matters, only the salient features will be discussed. The antenna consists of two pairs of dipoles in quadrature, with apertures of 20 feet. Either pair may be utilized for phase measurements. They are matched to a twin-channel receiver by 180-degree hybrids.

The receiver, a Racal R.153A, is phase and amplitude matched by manual compensation done with a variable delay line and a variable attenuator. The two signals from the receiver are branched into two paths to determine the variables necessary for solution of equation 13:

a. The signals are detected and differentially compared to determine $\left|V_1\right| - \left|V_2\right|$.

b. The signals are fed into the 90-degree hybrid, with $\left|V_3\right|$ and $\left|V_4\right|$ being detected at the output.

The three voltages are then processed by analog-to-digital converters for recording on magnetic tape.
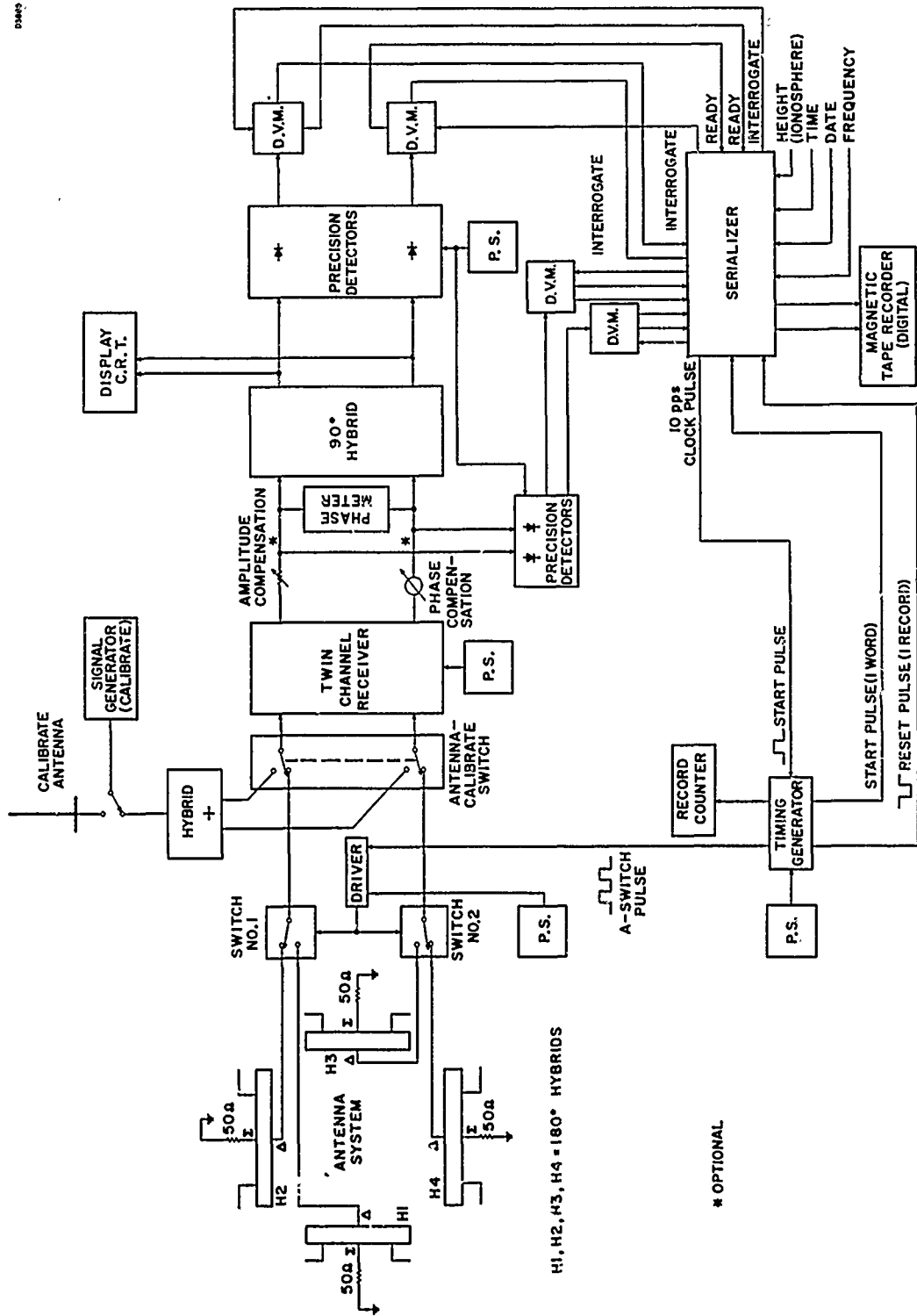
FIGURE 24 Data Collection Technique (U)

46

The serializer in Figure 24 locates and serializes the data flow onto the magnetic tape. After processing data fed to it by the analog-to-digital converters and channeling it to a magnetic tape recorder, the serializer interrogates the converters for new data and repeats the process to yield a new phase measurement. Each cycle requires 100 ms, limited by the time constant of the converters. Thus the system measures the phase, γ, at a rate of 10 samples per second. The magnetic tape is then processed by a Scientific Data Systems Model 930 computer utilizing a computer program.

There is also provision on the serializer for manual data to be read onto the tape prior to the phase measuring process. Manual data entered included frequency, time, date, and ionosphere height measured by an on-site ionosonde.

Standard procedure was to measure voltages for approximately one to two minutes and thereby enter several hundred successive measurements onto tape. The computer calculated the phases, printed them in time sequence, and averaged them. By rounding these phases to the nearest degree, a histogram was compiled and printed for comparison with the theoretical distributions presented in the last chapter.

This process was done twice for each experiment, first in the East-West dipoles, then on the North-South pair. Thus two average phases were generated, $2\psi_x$ and $2\psi_y$ respectively. Although it has been assumed in the previous chapter that the azimuthal angle, ϕ, was known, the two average phases provide both ϕ and θ of the stronger wave. Referencing ϕ to degrees east of north:

$$2\psi_x = \frac{2\pi a}{\lambda} \sin\theta_1 \sin\phi_1 \qquad \text{(East-West Pair)}$$

$$2\psi_y = \frac{2\pi a}{\lambda} \sin\theta_1 \cos\phi_1 \qquad \text{(North-South Pair)}$$

Dividing the first equation by the second and solving for the azimuthal angle:

$$\phi_1 = \tan^{-1}\left\{\frac{2\psi_x}{2\psi_y}\right\} \tag{14}$$

The elevation angle can be found as:

$$(2\psi_x)^2 + (2\psi_y)^2 = \left(\frac{2\pi a}{\lambda}\right)^2 \sin^2\theta_1 \ (\sin^2\phi_1 + \cos^2\theta_1)_.$$

$$\theta_1 = \sin^{-1}\left\{\frac{\left[(2\psi_x)^2 + (2\psi_y)^2\right]^{\frac{1}{2}}}{2\pi a/\lambda}\right\} \qquad (15)$$

Experimentation was limited to CHU, a station which transmits
time signals from Ottawa, Ontario, Canada. Located nearly due
north of Syracuse, CHU transmits a vertically polarized signal at
7.333 MHz with a radiated power output of 10 kilowatts. The re-
sults from experimentation with CHU transmission are shown in
Table 3, where they are compared with expected results. Since
the primary goal is elevation angle, resolution azimuthal results
are not included. The angles of arrival of the 1F and 2F modes
are expected to be near 27 degrees and 14 degrees, respectively,
assuming an F-layer height of 250 kilometers. Also, the 2F mode,
is expected to be, on the average, 18 dB below the 1F mode, cal-
culated using National Bureau of Standards attenuation procedures.
Hence, under normal conditions, it is expected that averaging
would yield the stronger ray.

Arbitrarily, relative errors in angle of arrival less than five per
cent will be considered satisfactory. In 61 per cent of the experi-
ments presented, the angles measured fell below this limit. The
histograms for these cases were very similar and a representative
pair from the March 27th experiment at 953 is presented in Figures
25 and 26. The phase distribution in Figure 25 was obtained from
the east-west pair of dipoles. Since CHU is nearly due north,
this pair is most sensitive to changes in ϕ. The average of this
distribution is 4.381 degrees, near which there is a peak. Also,
there is a peak on either side of this one.

According to the theoretical computer study conducted at SURC,
this distribution would represent amplitude variations with the
two predominant rays, 1F and 2F, arriving via different azimuthal
angles.

48

TABLE 3 Tabulation of Experimental Results

| Date	Time (hrs)	Ionospheric Height (km)	Angle of Arrival (degrees)	Per Cent Relative Error
1/29	1425	245	29.67	5.08
1/30	1043	220	31.27	0.95
1/30	1504	240	27.83	4.44
1/30	1513	240	31.61	11.21
3/5	1518	315	25.63	12.68
3/14	1513	250	31.78	16.37
3/20	1503	270	25.09	5.02
3/21	1625	250	34.03	26.68
3/22	1937	235	25.10	16.84
3/22	2010	245	24.49	15.81
3/25	934	255	27.54	0.03
3/25	949	255	28.56	4.36
3/25	1338	285	24.62	2.09
3/25	1400	285	30.42	25.09
3/25	1628	260	27.61	2.58
3/27	953	285	24.59	2.24
3/27	957	285	24.99	0.43
3/27	1138	260	27.61	2.58
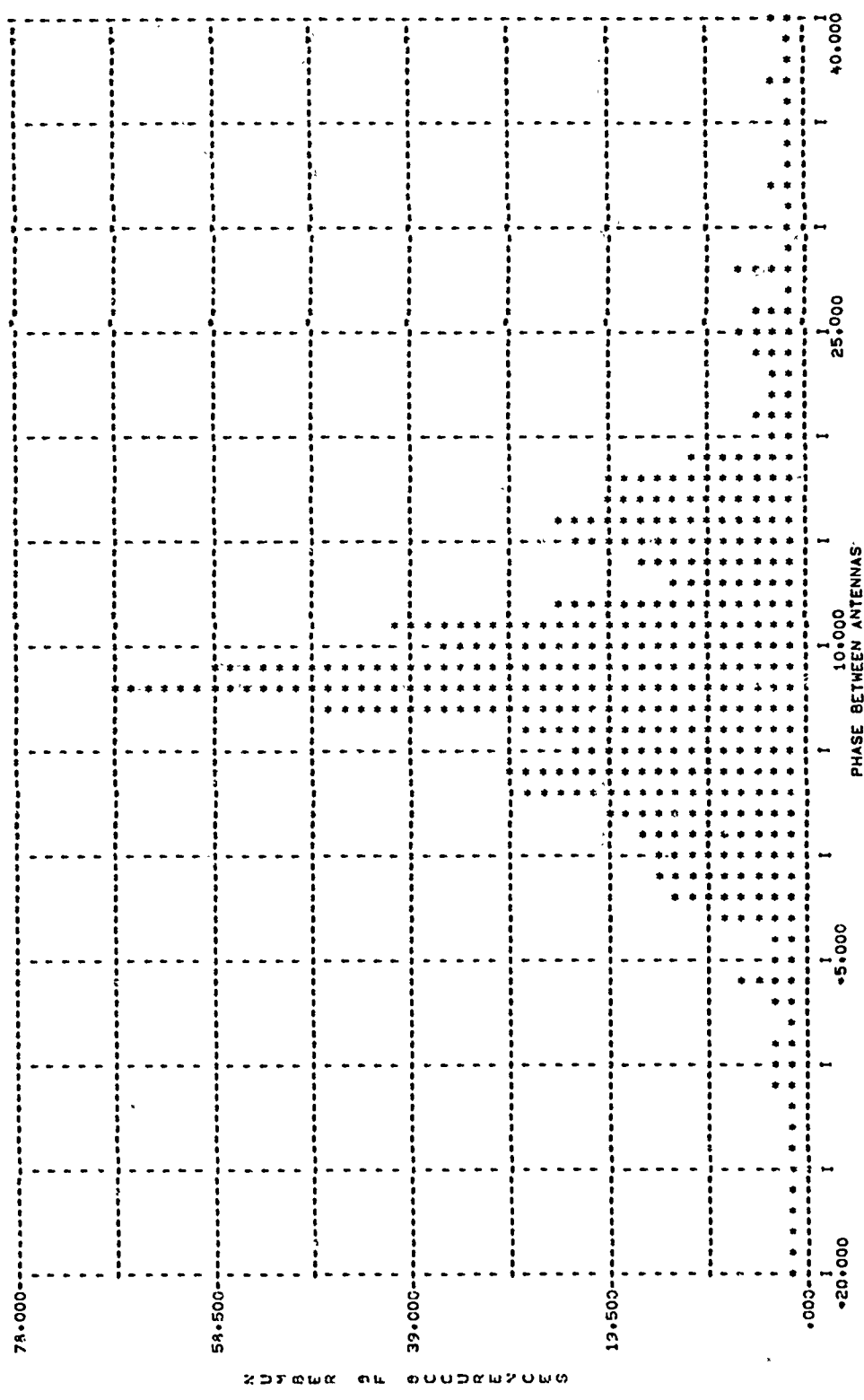
FIGURE 25 Experimental Phase Distribution East-West
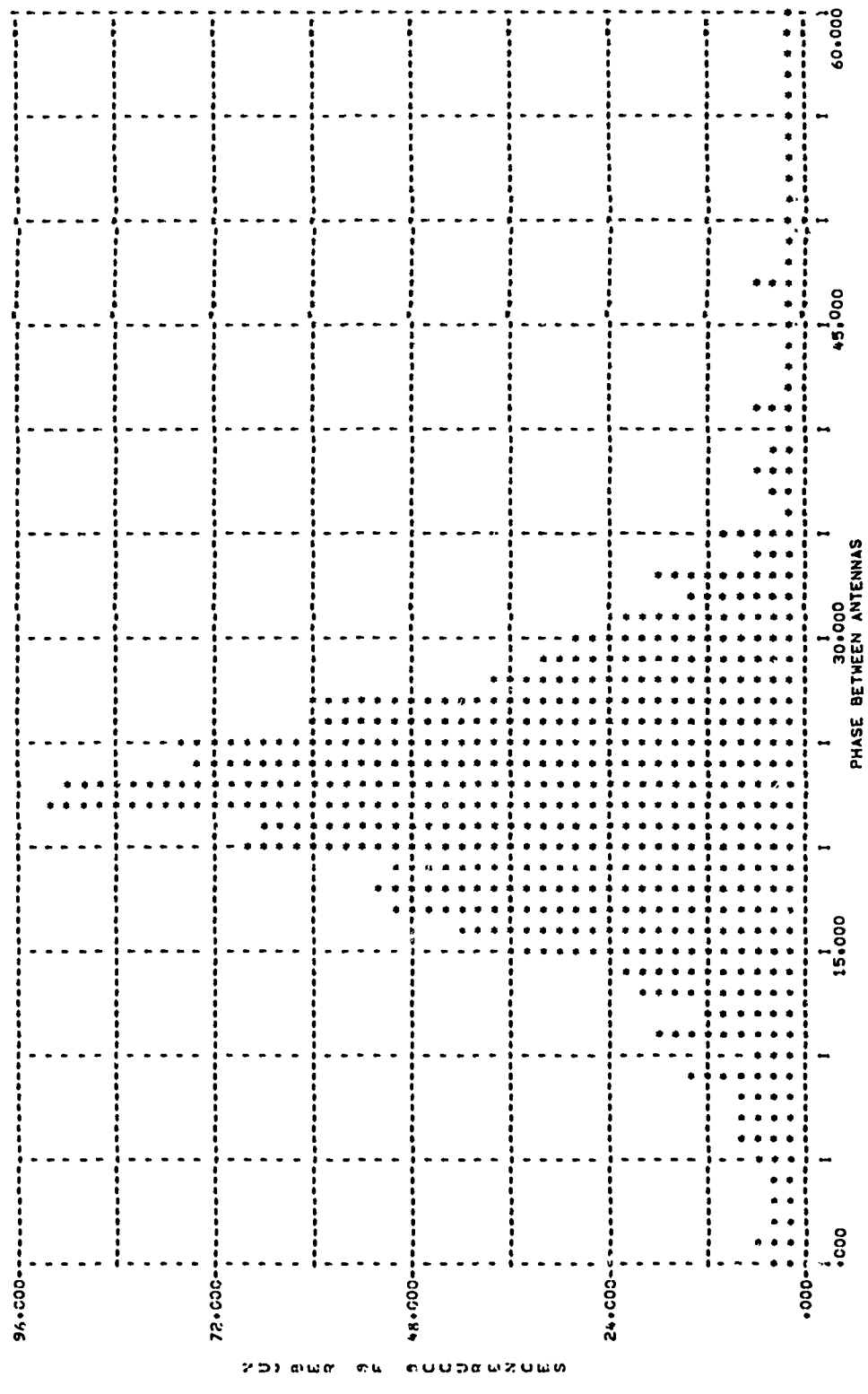Oriented Dipoles (U)

A6380

50

FIGURE 26 Experimental Phase Distribution North-South Oriented Dipoles (U)

A6381

51

Figure 26 shows the histogram obtained from readings on the north-south dipoles, which are phase dependent more on elevation angles of the incoming rays. This distribution bears a marked similarity to the theoretical distributions run on the computer lending some validity to the model adopted for variations in h and φ. The major difference appears to be the more Gaussian appearance of the experimental histogram. A plausible explanation for this may be found in the theory of random variables. According to the Central Limit Theorem, the more random variables that are allowed to affect a set of measurements, the more Gaussian will be the distribution of these measurements. In this problem, although only two interfering rays are considered, many more are actually present at the antenna much weaker than the two primary rays. Their presence would cause a minimal effect on averaging for the stronger ray, but their total influence would be to produce a more Gaussian appearing phase distribution.

More important features of the north-south distribution include the pronounced peak near the average of 21.88 degrees and the evidence of a weaker mode tending to widen the distribution below this value. To appreciate the value of time averaging, the wide variation in measured phases should be noted. An instantaneous measurement would yield an uncertain angle of arrival, possibly far from the angle corresponding to the stronger ray.

The distributions for experiments in which the error was greater were markedly different. The test on 22 March at 1937 hours is representative and the histograms are given in Figures 27 and 28. A general characteristic of the distributions in these cases is their higher dispersion, which indicates more severe interference. This is especially pronounced in Figure 28, the distribution most indicative of variations in elevation angle.

It was mentioned previously that on the average, the 2F mode would be 18 dB below the 1F, thus allowing very little chance for h to be greater than one under normal conditions. However, in the presence of localized ionospheric absorption, it is possible that the 1F mode may undergo additional attenuation causing the 2F mode to interfere more severely. In this way, many values of γ may be computed for which the 2F mode is stronger. This led to an error in the angle of arrival with respect to the normally predominant ray.
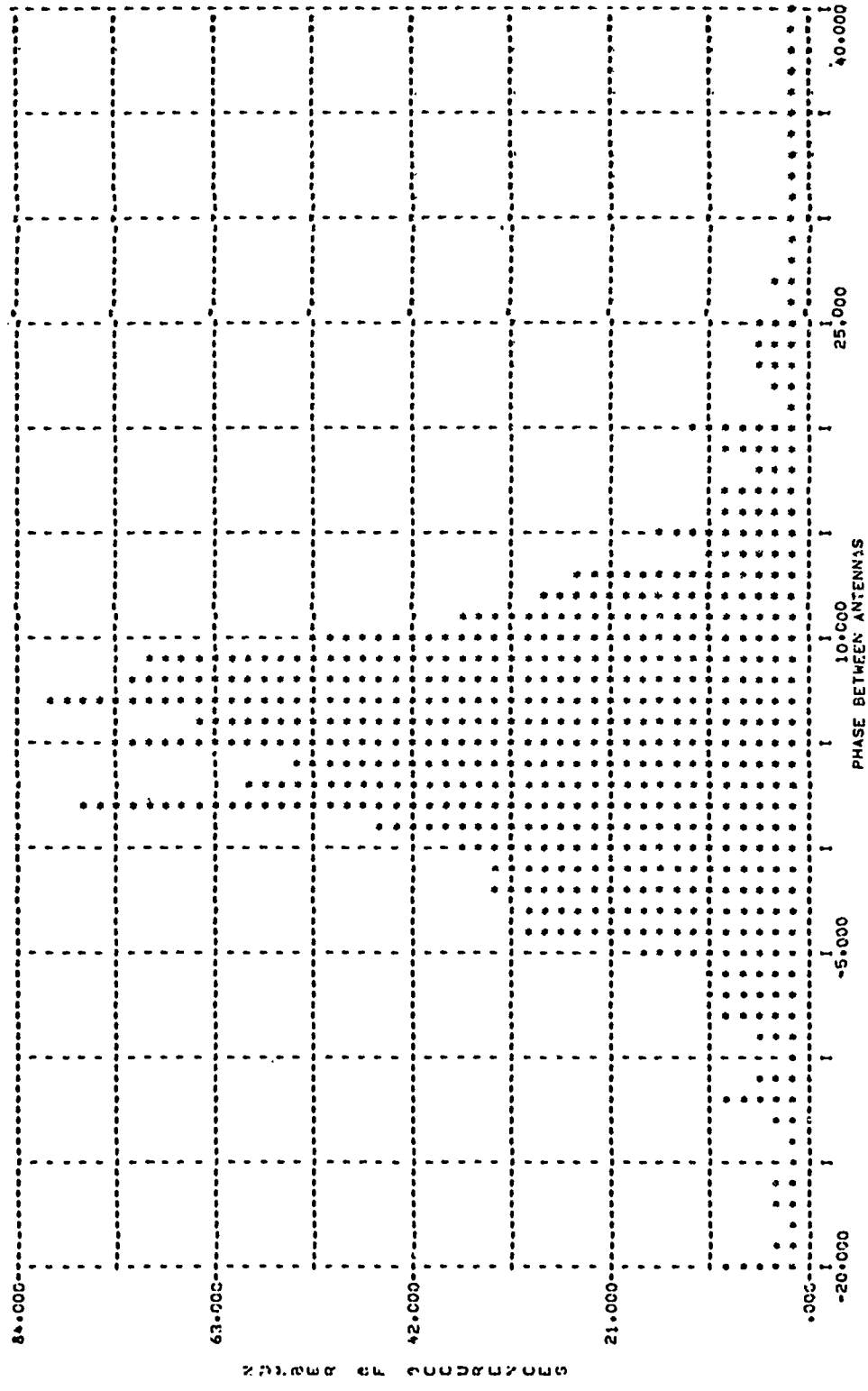
FIGURE 27   Experimental Phase Distribution East-West
Oriented Dipoles (U)
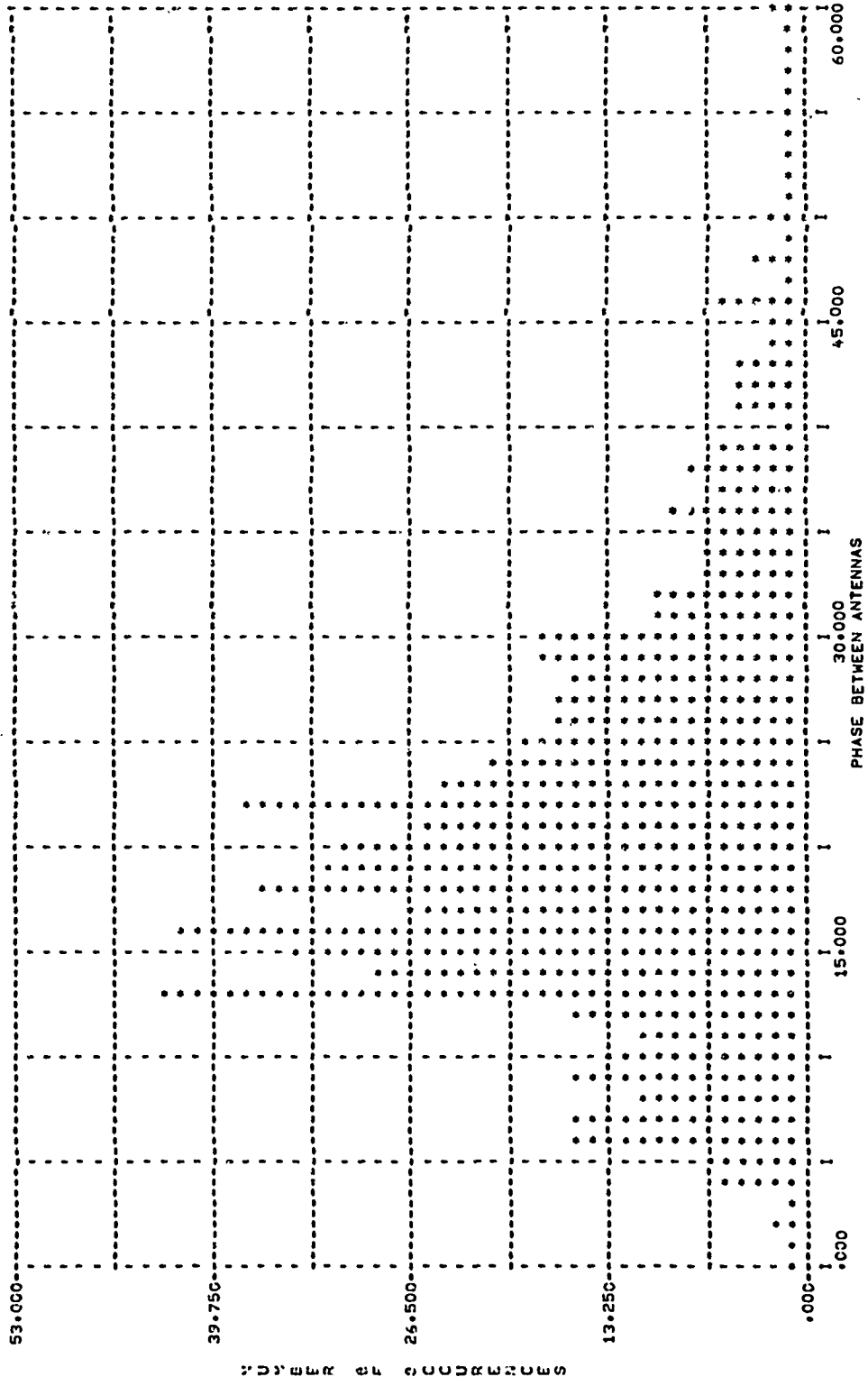
53

FIGURE 28   Experimental Phase Distribution North-South
Oriented Dipoles (U)

54

Referring to Figure 28, it appears that the 2F mode, near the peak at 13 degrees, figured significantly in the averaging, which yielded a phase below that associated with the 1F mode. Further evidence is afforded by the many values of phase located near the peak at 13 degrees.

Some experiments indicated an angle of arrival larger than that of the 1F mode. Examination of the ionograms for these cases often indicated the presence of an F_1 layer, which does not normally support a reflection. A wave reflected from this layer would arrive at an angle near 35 degrees and interfere severely. It is felt that this mode was present in these cases since an ionosonde return indicates probable oblique reflection from CHU.

On the whole, the initial experimental results are encouraging but much more investigation is necessary. The averaging process yields very good results when there is evidence from the histograms that the 1F mode is substantially stronger throughout the sampling time. In these cases, there is only a slight error due to averaging values of γ for which the 2F mode becomes predominant. However, one of the weaknesses of the procedure is a lack of reliability; that is, knowing when the conditions necessary for proper application of the time averaging theorem have been satisfied. This is due to an inability to recognize which is the primary ray when the phase is sampled. This will be studied in the follow-on work.

6.   TWIN FRONT END ALTERNATIVES STUDY (U)

The purpose of this study is to investigate the tradeoffs in twin front end design preference based on stated questionable factors for application in the Amphibious HF D/F System being developed at SURC.

The front end is to have simultaneously tuned channels for amplification of directional signal components in the high frequency range (0.5 to 20.0 MHz) without changing their relative amplitudes or phase.

There are three twin-front end system alternative approaches as shown in Figure 29.

```
                              |
                              |
                         ____/ _____
                        /                        \
                        |                         |
                   Distributed                    |
                   Front End                       |
                        |                           |
                    ___/ _____           |
                   /                      \          |
                   |                       |         |
              Matched              Unmatched        Lumped Front
              Channels             Channels with    End with Matched
                                   Calibration      Channels
```
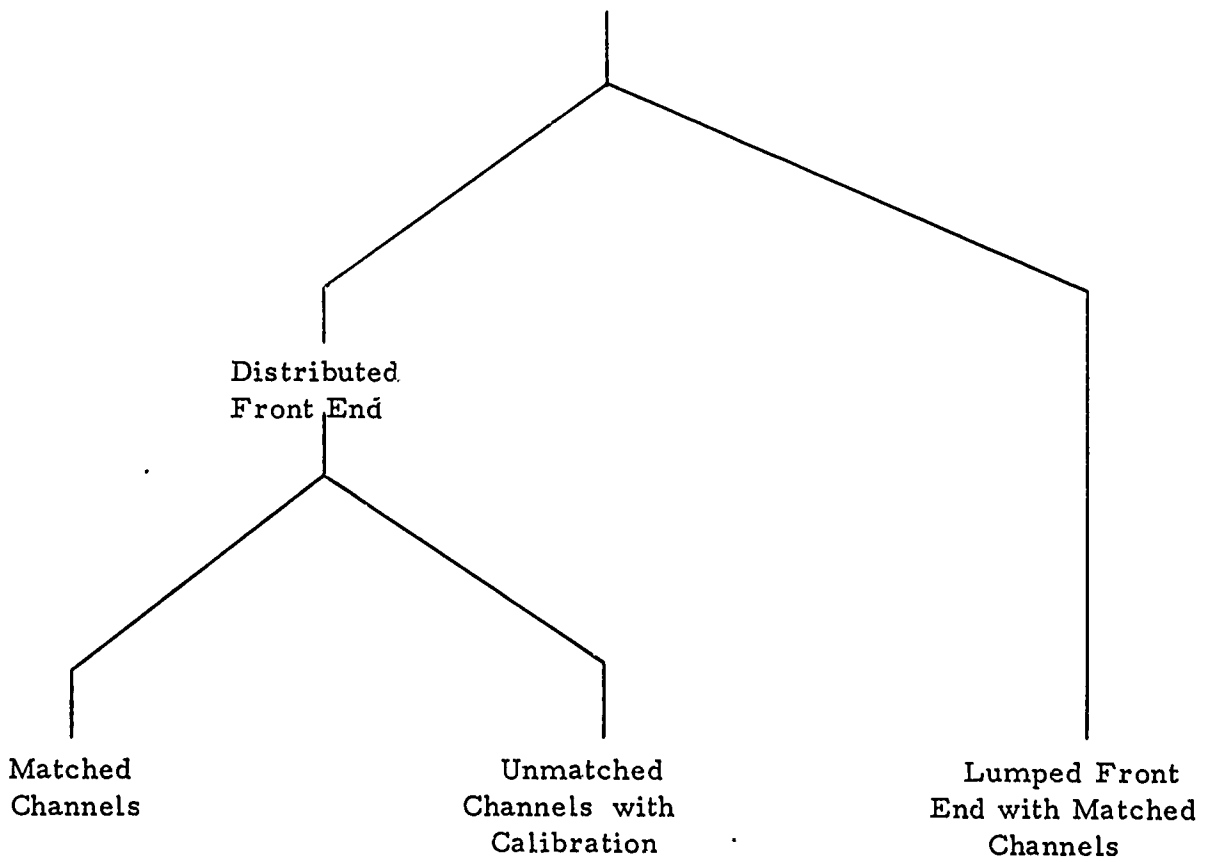
FIGURE 29   Twin Front End Alternatives (U)

a. <u>Twin Front End Design Preference (based only on operational desirability) versus Questionable Factors</u> (U)

The following table states the twin front end design preference and lists the questionable factors under each preference.

1st Choice -- Distributed Twin Front End with Matched Channels

Actual operational advantages

Technical feasibility

Cost and time constraints

Manufacturers acceptance of task

2nd Choice -- Distributed Twin Front End with Calibrated Unmatched Channels

Actual operational advantages

Technical feasibility

Cost and time constraints

3rd Choice -- Lumped Twin Front End with Matched Channels

Actual operational advantages

Cost and time constraints

b. <u>Evaluation of Twin Front End Techniques</u> (U)

The following factors will be considered and reported on as to technique and technical specification for each of the three system alternatives:

(1)   Channel amplitude and time delay tracking

(2)   Sensitivity

(3)   Dynamic range

(4)   Frequency control

(5)   Detection and signal processing

(6)   Spurious responses

(7)   Remote programming

(8)   Calibration

(9)   Human engineering

57

Special attention will be paid in reporting on the following main areas of interest:

(1) RF Processing

    (a) Input Stages

        Shall comment on devices used.

           Possible device:

               Parametric up converter

               Bi-polar transistor

               FET

    (b) RF Input Impedance

        Shall comment on input impedance specification and antenna impedance.

    (c) Noise Figure

        Shall comment on receiver noise figure specification for the three alternative systems.

    (d) Signal Handling Capability

        Shall comment on signal handling depending upon input devices used.

        Shall comment on weak signal optimization versus strong signal tradeoffs.

    (e) Tuning

        Shall study tuning technique to be used and time required to tune the receiver. Possible tuning techniques:

               Electronic (voltage tuned variactors)

               Broadband

               Mechanical

    (f) Spurious Response Suppression

        Shall comment on technical specifications for the following:

               Image Rejection

               Intermodulation products (state conditions)

               IF rejection

(2)   Frequency Control

All system alternatives will be capable of handling a minimum of two independent signal frequencies at the same instant of time. The technique for frequency control for each of the three system alternatives will be studied.

(a)   Digital Synthesizer

Phase lock loop

Integrated circuit reliability

10, 100, 1,000, 10,000 Hz channel spacing

Single crystal reference

Remote digital control available

Reduced spurious responses

(b)   Direct Synthesizer

High speed frequency switching

Interpolation in any decade increment

Remote control available

(c)   Hybrid Synthesizer

Low power consumption

Maximum flexibility

Electronic tuning

Frequency synthesizer constraints will be studied. (Injection level, impedance, spectral purity for local oscillator.)

Frequency read-out techniques will be studied.

(3)   Signal Processing and Detection

The Twin Front End system must be capable of detecting all types of modulation inherent in the HF frequency range of 0.5 to 30.0 MHz including AM, FM, USB, and LSB.

The last intermediate frequency shall be no lower than 455 kHz. The last IF bandwidths should be 800, 4,000 and 10,000 Hz. The desired shape factor of the IF filters is 4:1. (60 dB BW: 6 dB BW)

Linear phase characteristics in the last IF are desired.

Selectivity

Shall comment on the type of IF filters that will be used and the technical specifications that can be expected.

Heterodyne Scheme

Shall state the number of frequency conversions to be used.

Detectors

Shall be capable of demodulating the above mentioned modulations.

AGC

Shall comment on the following parameters, giving technical specifications where possible.

Dynamic range

Attack time

Decay times

AGC technique (IF, RF, LO control)

(4)   Miscellaneous

The portion of the Twin Front End system that is in the shelter will meet the temperature requirements of Mil E-16400, Class IV.

The portion of the Twin Front End system operated outside of the shelter will meet the temperature requirements of Mil E-16400, Class I.

Packaging

Shall comment on the packaging techniques that will be used in system fabrication.

Shall house the first stages of the front end at the antenna array in the distributed Twin Front End case. The last IF stage will be the first subsystem stage in the shelter.

Summary

Shall report the above parameters and techniques for each of the three system alternative approaches. Specifications and block diagrams of suggested systems will also be furnished in the study report.

Section III

FOLLOW-ON WORK PLAN (U)

Demonstration of feasibility in the three risk areas now permits a relatively straightforward approach to the accomplishment of formulating quantitative specifications for a complete improvement of the experimental system. The experimental system, as now envisioned, will include an array capable of narrow beam D/F on ground waves and/or single site fix on complex sky-waves. This array will consist of optimal feed networks, preamplifiers, and a Twin Front End with precision matching. The last section of the array will consist of electronic processing, analog-to-digital converters, and an RF calibration capability.

The shelter will accept the digital data inputs from the array and, utilizing near-real-time computer analysis, will retrieve fix and/or D/F information automatically. This information will be made available to the operator through computer print-out and visual displays. Other information generated includes polarization, frequency, demodulated signal, modulation mode, site assessment, D/F fix classification, and ionosonde information.

This follow-on work covers completion of the array portion of the system just discussed. Specific tasks to be accomplished under this effort are as follows:

a. An experimental program, involving testing of active elements with optimized feed networks and preamplifiers, will be conducted in order to determine the final array configuration. This program will include computer analysis and propagation testing.

b. In order to determine optimal time convergence of sampling, sampling rate, time per unit sample, and fade spectrum, further propagation tests will be run. These tests will also add additional range and seasonal propagation information to the propagation data base already obtained.

c. Based on the information obtained in the preceding task, array processing electronics will be designed and fabricated.

d. A developmental test model of the twin front end electronics will be designed and fabricated for use in the array.

GLOSSARY (U)

1, 2	Subscripts 1, 2 refer to waves A and B, respectively.
Re	The real part of.
Im	The imaginary part of.
A_ϕ, A_θ	The projection of the magnitude of the electric or magnetic field vector associated with wave A propagating in direction $\vec{k}_1$.
B_ϕ, B_θ	Corresponding definition for wave B.
$\vec{k}_{1,2}$	$k(\cos\alpha_{1,2}\ \underline{u}_x + \cos\beta_{1,2}\ \underline{u}_y + \cos\gamma_{1,2}\ \underline{u}_z)$.
k	$2\pi/\lambda$, λ being the free space wavelength.
$\cos\alpha_{1,2}$	The direction cosine with respect to the x-axis.
$\cos\beta_{1,2}$, $\cos\gamma_{1,2}$	Corresponding definition for the other axis.
$\underline{u}_\theta$, $\underline{u}_\phi$, $\underline{u}_x$, $\underline{u}_y$, $\underline{u}_z$	Unit vectors directed toward positive direction of the subscripted coordinate.
$\delta_{1,2}$	The time phase difference between A_θ and A_ϕ or B_θ and B_ϕ.
$\beta(t)$	The time phase difference between the two waves.
$\vec{r} = x\underline{u}_x + y\underline{u}_y + z\underline{u}_z$	The radius vector.
$\psi_{1,2} = ka\sin\theta_{1,2}\cos\Phi_{1,2}$	

65

PERSONNEL (U)

G. H. LaTourette, Director, Surface Signal Laboratory

R. G. Russell, Project Engineer

R. L. Brennan, Research Engineer

S. E. Cooper, Research Engineer

H. A. Schuman, Research Engineer

T. J. Carter, Technician

E. E. Gay, Technician

DOCUMENT CONTROL DATA - R&D

(Security classification of title, body of abstract and indexing annotation must be entered when the overall report is classified)

1. ORIGINATING ACTIVITY (Corporate author)	2a. REPORT SECURITY CLASSIFICATION
Defense Systems Division	UNCLASSIFIED
Syracuse University Research Corporation	2b. GROUP
Merrill La./Univ. Hgts., Syracuse, N.Y. 13210	N/A

3. REPORT TITLE

ANTENNA STUDY FOR D/F APPLICATION

4. DESCRIPTIVE NOTES (Type of report and inclusive dates)

Semi-Annual Progress Report 1968 January 1 to 1968 June 30

5. AUTHOR(S) (Last name, first name, initial)

Russell, R. G. , Cooper, S. E. , Schuman, H. A.

6. REPORT DATE	7a. TOTAL NO. OF PAGES	7b. NO. OF REFS
1968 November	82	7

8a. CONTRACT OR GRANT NO.	9a. ORIGINATOR'S REPORT NUMBER(S)
NOnr 4798(00)	DSD R-219
b. PROJECT NO.	
CS 454 and CS 471	
c.	9b. OTHER REPORT NO(S) (Any other numbers that may be assigned this report)
d.	NONE

10. AVAILABILITY/LIMITATION NOTICES

"Each transmittal of this document outside the Department of Defense must have prior approval of the Chief of Naval Research (Code 463) Washington, D.C. 20360."

11. SUPPLEMENTARY NOTES	12. SPONSORING MILITARY ACTIVITY
NONE	Office of Naval Research
	Department of the Navy

13. ABSTRACT

The feasibility of utilization of a short dipole, elevated array has been demonstrated on ground-wave signals and sky-wave signals. The feasibility of sky-wave ranging has also been demonstrated. Theoretical and experimental results are included.

A data package has been submitted for the Interim Replacement for the AN/TRD-21 Antenna System.

DD FORM 1473 1 JAN 64

Security Classification

14.		LINK A		LINK B		LINK C	
KEY WORDS		ROLE	WT	ROLE	WT	ROLE	WT
AN/TRD-21 Replacement							
Elevation angle							
Direction finding							
Sky-wave							
Wave interference							
Ionosphere							
Time averaging							
Active elements							

INSTRUCTIONS

1. ORIGINATING ACTIVITY: Enter the name and address of the contractor, subcontractor, grantee, Department of Defense activity or other organisation (corporate author) issuing the report.

2a. REPORT SECURITY CLASSIFICATION: Enter the overall security classification of the report. Indicate whether "Restricted Data" is included. Marking is to be in accordance with appropriate security regulations.

2b. GROUP: Automatic downgrading is specified in DoD Directive 5200.10 and Armed Forces Industrial Manual. Enter the group number. Also, when applicable, show that optional markings have been used for Group 3 and Group 4 as authorized.

3. REPORT TITLE: Enter the complete report title in all capital letters. Titles in all cases should be unclassified. If a meaningful title cannot be selected without classification, show title classification in all capitals in parenthesis immediately following the title.

4. DESCRIPTIVE NOTES: If appropriate, enter the type of report, e.g., interim, progress, summary, annual, or final. Give the inclusive dates when a specific reporting period is covered.

5. AUTHOR(S): Enter the name(s) of author(s) as shown on or in the report. Enter last name, first name, middle initial. If military, show rank and branch of service. The name of the principal author is an absolute minimum requirement.

6. REPORT DATE: Enter the date of the report as day, month, year; or month, year. If more than one date appears on the report, use date of publication.

7a. TOTAL NUMBER OF PAGES: The total page count should follow normal pagination procedures, i.e., enter the number of pages containing information.

7b. NUMBER OF REFERENCES: Enter the total number of references cited in the report.

8a. CONTRACT OR GRANT NUMBER: If appropriate, enter the applicable number of the contract or grant under which the report was written.

8b, 8c, & 8d. PROJECT NUMBER: Enter the appropriate military department identification, such as project number, subproject number, system numbers, task number, etc.

9a. ORIGINATOR'S REPORT NUMBER(S): Enter the official report number by which the document will be identified and controlled by the originating activity. This number must be unique to this report.

9b. OTHER REPORT NUMBER(S): If the report has been assigned any other report numbers (either by the originator or by the sponsor), also enter this number(s).

10. AVAILABILITY/LIMITATION NOTICES: Enter any limitations on further dissemination of the report, other than those imposed by security classification, using standard statements such as:

(1) "Qualified requesters may obtain copies of this report from DDC."

(2) "Foreign announcement and dissemination of this report by DDC is not authorized."

(3) "U. S. Government agencies may obtain copies of this report directly from DDC. Other qualified DDC users shall request through

_____."

(4) "U. S. military agencies may obtain copies of this report directly from DDC. Other qualified users shall request through

_____."

(5) "All distribution of this report is controlled. Qualified DDC users shall request through

_____."

If the report has been furnished to the Office of Technical Services, Department of Commerce, for sale to the public, indicate this fact and enter the price, if known.

11. SUPPLEMENTARY NOTES: Use for additional explanatory notes.

12. SPONSORING MILITARY ACTIVITY: Enter the name of the departmental project office or laboratory sponsoring (paying for) the research and development. Include address.

13. ABSTRACT: Enter an abstract giving a brief and factual summary of the document indicative of the report, even though it may also appear elsewhere in the body of the technical report. If additional space is required, a continuation sheet shall be attached.

It is highly desirable that the abstract of classified reports be unclassified. Each paragraph of the abstract shall end with an indication of the military security classification of the information in the paragraph, represented as (TS), (S), (C), or (U).

There is no limitation on the length of the abstract. However, the suggested length is from 150 to 225 words.

14. KEY WORDS: Key words are technically meaningful terms or short phrases that characterize a report and may be used as index entries for cataloging the report. Key words must be selected so that no security classification is required. Identifiers, such as equipment model designation, trade name, military project code name, geographic location, may be used as key words but will be followed by an indication of technical context. The assignment of links, rules, and weights is optional.

DD FORM 1 JAN 64 1473 (BACK)